

**EFFECTS OF ALUMINUM FIN THICKNESS COATED WITH A SOLAR
PAINT ON THE THERMAL PERFORMANCE OF EVACUATED TUBE
COLLECTOR (ETC)**



**A Thesis Submitted to the Graduate School of Naresuan University
in Partial Fulfillment of the Requirements
for the Master of Science Degree in Renewable Energy**

June 2017

Copyright 2017 by Naresuan University


Thesis entitled "Effects of Aluminum Fin Thickness Coated with a Solar Paint on
the Thermal Performance of Evacuated Tube Collector"


By Mr. Amanuel Andemeskel Haile

has been approved by the Graduate School as partial fulfillment of the requirements
for the Master of Science Degree in Renewable Energy of Naresuan University

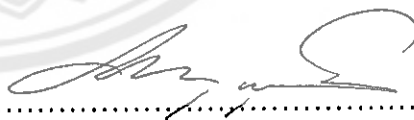
Oral Defense Committee

.....  Chair
(Associate Professor Sirichai Thepa, D.Sc.)

.....  Advisor
(Assistant Professor Tawat Suriwong, Ph.D.)

.....  Internal Examiner
(Assistant Professor Sarayooth Vaivudh, Ph.D.)

Approved

..... 
(Panu Putthawong, Ph.D.)

Associate Dean for Administration and Planning
for Dean of the Graduate School

- 9 JUN 2017

ACKNOWLEDGEMENT

First I would like to thank my advisor Assistant Professor Dr. Tawat Suriwong. He was greeting me with delight whenever I have question or doubt about the thesis. His continuous dedication in supporting the thesis makes me to accomplish the work on time.

I would also like to thank to TICA, who provides me the scholarship. And other experts and staff member of School of Renewable Energy, Naresuan University, for their support and motivation.

My heartfelt thanks to the committee member for their valuable suggestions on gaining approval of my thesis.

Finally, I must express my very profound gratitude to my spouse and family member for providing me with unfailing support and continuous encouragement throughout my years of study. This accomplishment would not have been possible without them.

Amanuel Haile

Title EFFECTS OF ALUMINUM FIN THICKNESS COATED
WITH A SOLAR PAINT ON THE THERMAL
PERFORMANCE OF EVACUATED TUBE COLLECTOR

Author Amanuel Haile

Advisor Assistant Professor Tawat Suriwong, Ph.D.

Academic Paper Thesis Msc. In Renewable Energy,
Naresuan University, 2016

Keywords Evacuated tube collector (ETC), solar paint, aluminum fin,
thermal efficiency, solar absorptance.

ABSTRACT

In commercial evacuated tube collector (ETC) with double layers evacuated tube, a solar absorber is coated on outer surface of the inner glass vacuum tube. In order to reduce cost of production and maintenance, our previous research work has been successfully initiated to place an aluminum fin inside the ETC to be a solar receiver together with clear double layers evacuated tube. Therefore, the objective of this present research is focused on the effect of aluminum (Al) fin thickness coated with solar paint on the thermal performance of ETC. Commercial Al fins with three different thicknesses (11, 13, and 24 μm) were considered in this study. An available solar paint (with a trade name-Thurmolax 250) was coated on the Al fin solar absorber using an air spray deposition technique with three different coating thicknesses. Phase, reflectivity and thickness of the coatings were characterized using X-ray Diffraction (XRD), Ultraviolet-visible-near infrared (UV-Vis-NIR) spectrophotometer at the wavelengths 300-2500 nm and a Mini Test 730 equipment respectively. The solar absorptance (α) was calculated based on the relationship of observed reflectivity (R), and the solar spectral irradiance of AM 1.5 in the whole wavelength range of solar spectrum. The collector thermal efficiency (η) of ETC with different thicknesses of Al fin coated with solar paint as solar receiver was evaluated, following a standard ISO 9806-1. As a result, it is found that the α of all the thicknesses of solar paints considered was identical ($\alpha=0.94$), indicating that the thickness of solar paint was an insignificant effect on the α . The η , heat removal factor (F_R), and overall heat loss

coefficient (U_L) were calculated for different Al fin thicknesses with same coating thickness and were found to be increasing with decreased Al fin thickness. The results revealed that the F_R was predominant for the increase in the η with the reduction of Al fin thickness. It can be concluded that thinner Al fin with single layer solar paint coating is suggested to be used in ETC due to its higher η and F_R , including light weight and low cost.



LIST OF CONTENTS

Chapter	Page
I INTRODUCTION.....	1
Rationale for the study and statement of the problem	1
Objective of the study.....	2
Scope of the study.....	3
Benefits of the study.....	3
II REVIEW OF RELATED LITERATURE AND RESEARCH....	4
Solar Thermal Collectors.....	4
Evacuated Tube Collector (ETC).....	5
Solar Selective Surface.....	8
Coating.....	10
Painting.....	11
Thermal Performance.....	11
Economical Evaluation.....	14
Literature Review.....	15
III RESEARCH METHODOLOGY.....	22
Research Area.....	22
Equipment and Material Used.....	22
Coating of Al with solar paint.....	22
Characterization of samples.....	24
Outdoor testing of ETC and experiment condition.....	26
Calculation and Analysis.....	28
Levelized cost of energy (LCOE).....	28
Procedure and Methodology.....	30

LIST OF CONTENTS (CONT.)

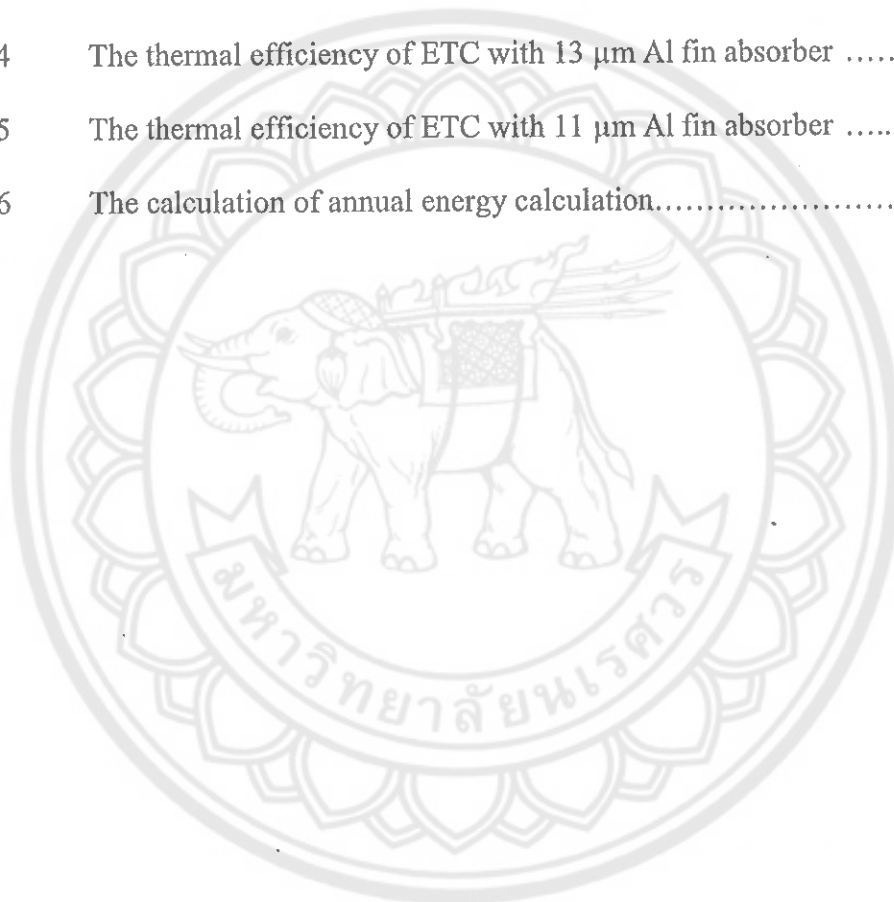
Chapter	Page
IV RESULT AND DISCUSSION.....	31
Determination of coating thicknesses.....	31
Ultraviolet-Visible- Near Spectrophotometer analysis.....	33
X-ray Diffraction analysis.....	35
Evaluation of thermal efficiency of the ETC.....	36
Evaluation of LCOE for ETC using different Al fin thickness...	39
V CONCLUSION.....	45
Conclusions.....	45
Recommendations.....	47
REFERENCES.....	48
APPENDIX.....	53
BIOGRAPHY.....	78

LIST OF TABLES

Table	Page
1 Solar Energy Collectors	4
2 Summary of the Literature Review	18
3 Composition of Al.....	22
4 Properties of thurmalox 250 black solar paint	23
5 Collector specification.....	26
6 Tolerance of measured parameters.....	27
7 R and α of the three different painting thickness	34
8 General equation of ETC.....	37
9 Comparison of thermal efficiency equations	38
10 Investment cost and benefit of the project	40
11 Parameters for calculation.....	41
12 Values of parameters for calculating the energy yield.....	41
13 Annual yield energy from ETC.....	42
14 The LCOE of the ETC using Al fin of 11 μm thickness as solar absorber	43
15 The LCOE of the ETC using Al fin of 13 μm thickness as solar absorber	44
16 The LCOE of the ETC using Al fin of 24 μm thickness as solar absorber	45
17 Paint thicknesses different position for sample of single layer coating.....	53
18 Paint thicknesses different position for sample of double layer coating.....	54
19 Paint thicknesses different position for sample of triple layer coating.....	55
20 The calculation of the solar absorptance of solar paint coated Al fin single layer	61

LIST OF TABLES (CONT.)

Table		Page
21	The calculation of the solar absorptance of solar paint coated Al fin double layer	63
22	The calculation of the solar absorptance of solar paint coated Al fin triple layer	65
23	The thermal efficiency of ETC with 24 μm Al fin absorber	67
24	The thermal efficiency of ETC with 13 μm Al fin absorber	70
25	The thermal efficiency of ETC with 11 μm Al fin absorber	73
26	The calculation of annual energy calculation.....	76



LIST OF FIGURES

Figures	Page
1 Cross section of commercial evacuated tube showing original coating	2
2 Types of solar collectors	5
3 (a) Evacuated tube solar collector and (b) inside part of the evacuated tube glass	6
4 Inside part of ETC	7
5 Solar spectral irradiance for AM ⁰ 1.5.....	9
6 Performance curve of ETC.....	13
7 Open loop test system	14
8 a) Cross section of new coating b) Coating on Aluminum fin solar absorber	23
9 Digital mini Test 730	24
10 Rigaku miniflex II X-ray diffraction	25
11 Ultraviolet-Visible-Near Infrared Spectrophotometer	25
12 (a) Equipment setup and (b) its equivalent schematic diagram ...	27
13 Components of LCOE.....	29
14 Flow Chart of Procedure and methodology of the study.....	30
15 Histogram curve of solar paint thickness for single layer coating.	31
16 Histogram curve of solar paint thickness for double layer coating	32
17 Histogram curve of solar paint thickness for triple layer coating..	33
18 Spectral reflectance (R) and solar absorptance (α) curves of coated Al solar absorber comparing with the sun spectrum at AM 1.5 in the wavelength interval 300-2500 nm for single (1x), double (2x) and triple (3x) layer coated Al absorber fin.....	34
19 XRD pattern of solar paint coated Al and Al fin	35

LIST OF FIGURES (CONT.)

Figures		Page
20	Comparison of performance curve of ETC using Al fin thickness of 11, 13 and 24 μm as the solar absorber.....	36
21	η versus Al fin solar absorber thicknesses of the ETC curve	37



ABBREVIATION

α	Absorptance
$R(\lambda)$	The spectral reflectance, measured at a specific wavelength, λ
I_s	The solar spectra radiation (W/(m ² ·m))
λ_1, λ_2	Wave length range (m)
η	Thermal Collector Efficiency
Q_u	Useful energy gain from the collector (W)
$(\tau\alpha)_n$	Normal transmittance absorptance product
$F_R(\tau\alpha)_n = c_o$	The intercept (intersection of the line with the vertical efficiency axis)
$F_R U_L$	The slope of the line
T_i	Inlet fluid temperature at the collector inlet (°C)
T_o	Out let fluid temperature at the collector outlet (°C)
T_a	Ambient air temperature (°C)
c_1 and c_2	First and second order heat loss coefficients
c_p	specific heat of water at constant pressure (J/(kg·°C))
\dot{m}	Mass flow rate of water (kg/s)
G_t	Global solar radiance at the collector plane (W/m ²)
C_c	Initial capital cost
C_n	Operating cost
E_n	Energy produced each year (kWh)
i	Interest rate of discount rate
n	Project period
N	Year at the end of the project

CHAPTER I

INTRODUCTION

Rational for the study and statement of the problem

As the need of thermal energy worldwide increases from time to time, improving thermal efficiency of solar collector become very crucial and indispensable. Efficiency of device or a system is improved mainly by increasing the efficiency or effectiveness of its components. According to the previous study, solar absorber is one part of solar collector which has a great roll on the performance of the solar collector. Solar paint, solar absorber material, and absorber topology or absorber geometry have great influence on the thermal performance of solar absorber. Various researchers have contributed in improving the thermal performance of solar collector by using polymers and nanofluids for reducing weight and increasing the thermal conductivity, and also material modification by improving material producing techniques. [1, 2, 3].

Numerous solar collectors are used in this world; their classification is mainly based on its design. Evacuated Tube Collector (ETC) is the most efficient and convenient collector among various kinds of solar collectors [4].

One of the main important part of a collector is the fin absorber, and this part has a significant influence on collector performance, like its surface area, coating thickness, material and solar coating type [4, 5]. As the heat transfer rate is affected by the thickness of material (from the basic conduction heat formula), the performance of the ETC is expected to vary as the thickness of the absorber material is varied.

Spectral selectivity surface is affected by the substrate reflectance and the painting method used to. Solar paint is one of the solar selective coating with lower cost and easy to apply. As the absorber substrate material and solar paint coating thickness varies, the absorber cost will also vary accordingly and this change might reflect on the levelized cost of energy (LCOE).

The commercial available ETC requires highly technique to apply the coating, as the coating is in the inner part of the glass tube as shown in the figure 1;

once the glass tube broken, the whole glass tube with coating should be replaced and this will increase the maintenance cost.

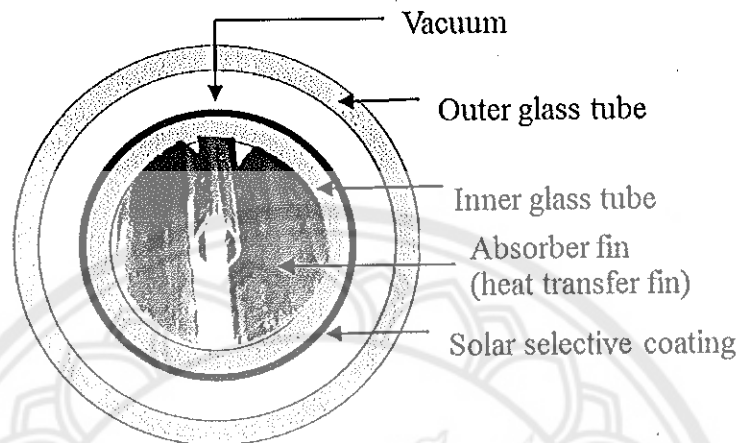


Figure 1 Cross section of commercial evacuated tube showing original coating

In present study, therefore, solar paint coating on aluminum absorber fin of ETC will be used. And effects of the thickness of aluminum fin absorber coated with a solar paint on the thermal performance of ETC will be studied. Moreover, levelized cost of energy will be evaluated in order to determine the cost of the system per total energy produced and compare among their types of ETC.

Objectives of the study

1. To investigate the characteristics and phase of various solar paint coating thickness on aluminum fin absorber plate.
2. To determine the thermal performance of ETC with various solar paint coated aluminum fin absorber thickness.
3. To evaluate the Levelized Cost Of Energy (LCOE) of ETC used in solar water heating system.

Scope of the study

1. Selective solar collector coating (Thermalox 250 selective black solar collector coating, Dampney Company) will be applied to aluminum fin with different coating thickness.

2. Investigation of reflectance, phase and solar coating thickness of solar paint applied on aluminum fin samples by UV-Vis-NIR Spectrophotometer, XRD, and Electro Physic Min Test 730 respectively.

3. Applying the solar paint to the three different aluminum fin thickness. (0.11, 0.13, and 0.24mm).

4. Carrying out of outdoor experiment (School of Renewable Energy Technology, Naresuan University) for the determination of thermal performance of different aluminum fin absorber thickness.

5. To evaluate the Levelized Cost of Energy (LCOE) based on the cost of the ETC system per total energy produced.

Benefits of the study

1. To get a relation between efficiency and the aluminum fin thickness that will be a base for further research.

2. All the commercial and small scale end users of these system will have benefit from this study.

CHAPTER II

REVIEW OF RELATED LITERATURE AND RESEARCH

Solar Thermal Collector

It is a device that collects solar energy and change to thermal energy by exposing the collector to the sun shine. The function of the collector system is to heat a fluid passing through the conduit by converting incident solar radiation into thermal energy with minimum heat losses [6]. There are basically two types of collectors, stationary and tracking. Stationery collectors classify further as shown below in table 1(with their indicative temperature) and Figure 2.

Table 1 Solar Energy Collectors [7]

Motion	Collector Type	Absorb er type	Concentratio n ratio, C	Indicative temperatu re range(°C)
Stationery	Flat-plate collector (FPC)	Flat	1	30-80
	Evacuated tube collector (ETC)	Flat	1	50-200
	Compound parabolic Collector (CPC)	Tabular	1-5	60-240
Single- axis tracking	Linear Fresnel collector (LFR)	Tabular	5-15	60-300
	Cylindrical trough collector	Tabular	10-40	60-250
	Parabolic trough collector (PTC)	Tabular	15-50	60-300
			10-85	60-400
Two- axis tracking	Parabolic dish reflector(FDR)	Point	600-2000	100-1500
	Heliostat field collector (HFC)	Point	300-1500	150-2000

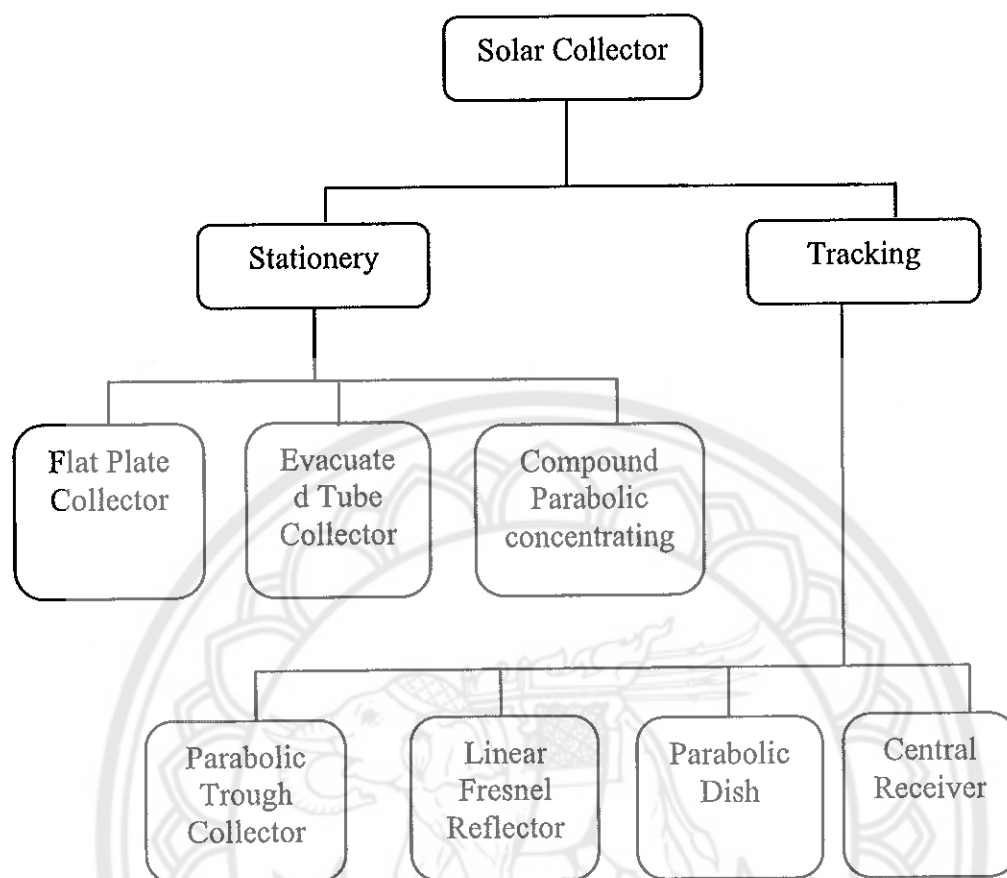


Figure 2 Types of solar collectors [8]

Evacuated Tube Collector (ETC)

It is one type of solar collector which uses heat pipe, absorber plate enclosed in double sealed evacuated glass as shown in Figure 3 and 4. The heat pipe is made of copper and has fluid on it. The ETC converts energy from the solar energy into usable thermal energy. ETC operates differently when it compares with the other collectors available on the market. These solar collectors consist of a heat pipe inside a vacuum-sealed tube, as shown in Figure 3. In an actual installation, many tubes are connected to the same manifold [7].

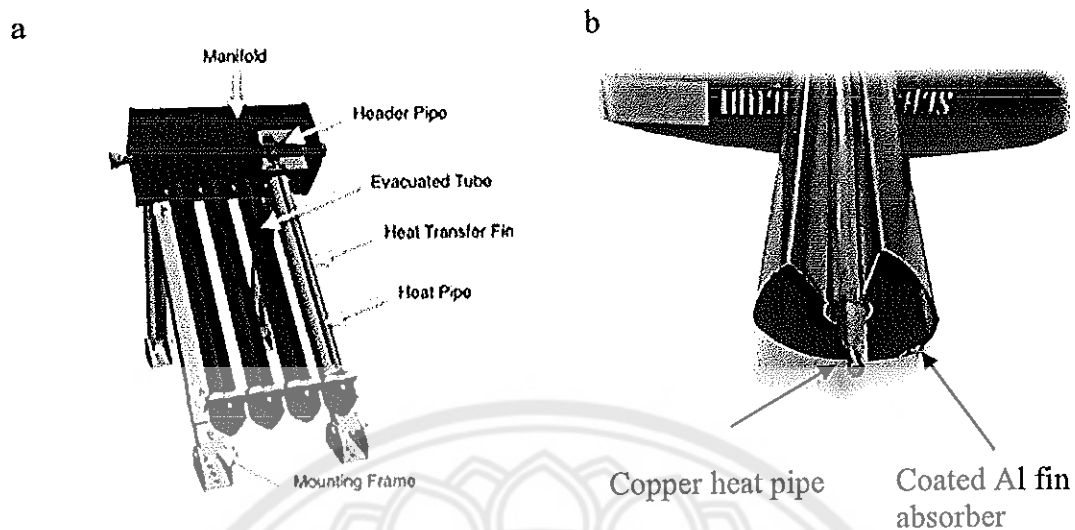


Figure 3 (a) Evacuated tube solar collector [9] and (b) inside part of the evacuated tube glass

The ETCs minimize convective heat loss by placing the solar absorbing surface in a vacuum. Radiation heat loss is also minimized by using a low emissivity absorber surface [10]. Some of the advantages of the heat pipe evacuated tubular solar collectors are anti-freezing, rapid start-up, resistance to high pressure, easy installation and maintenance. But the heat pipe evacuated tubular must maintain the vacuum environment [11]. It has more benefit than the FPC, as it uses vacuum glass tube to reduce the heat loss through conduction and convection. ETCs are used in small and large of sea water desalination, air conditioning, building heating, refrigeration, and higher temperature production for industrial application [8]. According to many researchers [7, 10] ETC have much higher efficiencies than FPCs. ETC can collect both direct and diffuse radiations, excellent thermal performances and convenient installation and easy transportability.

Heat energy can be extracted from evacuated tube in different methods namely: 1) using heat pipe, 2) flow through absorber, 3) all glass tubes and 4) storage absorber [10].

ETC consists of a heat pipe kept inside a glass enclosure, as shown in Figure 4. The heat pipe uses liquid to capture heat of solar insolation and this liquid transfers heat to some other working fluid while undergoing evaporation–condensation cycles.

On receiving solar radiation, the liquid inside the heat pipe undergoes phase change and it is converted into vapor, which rises toward the upper part of the heat pipe due to buoyancy. The vapor condenses back to liquid after transferring heat to the working fluid in the heat exchanger section at the top. The liquid flows back to the bottom of heat pipe due to gravity, and the cycle continues. The glass enclosure is evacuated to minimize the heat loss due to convection and to prevent climatic degradation of its inner materials. Generally, heat pipes are also evacuated to allow phase change of the inner liquid at low temperatures. Its efficiency is not significantly affected by change in incidence angle of sun's radiation. This feature of ETC provides flexibility to tube orientation from 25° to 60° at the time of installation [5].

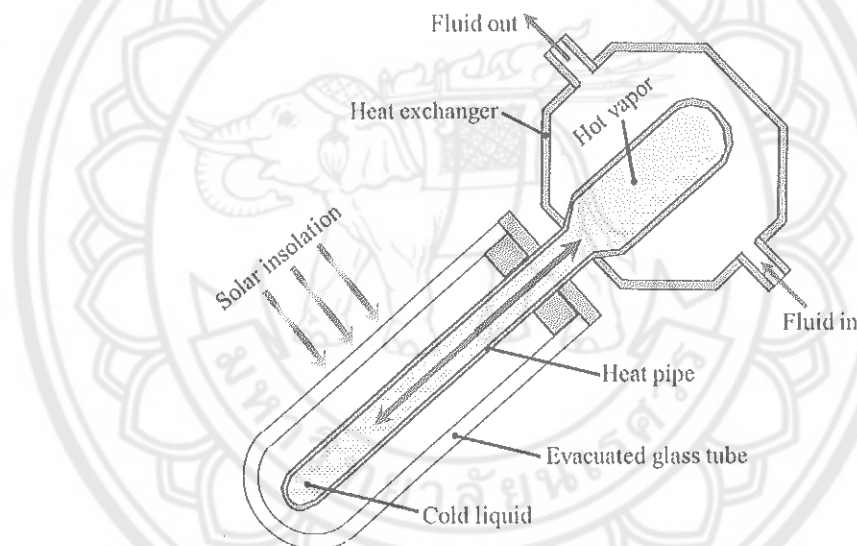


Figure 4 Inside part of ETC [5]

The process in the evacuated tube is operated by fluid flowing through the absorber and it can be collected the heat by means of the heat pipe principle. There is a small amount of fluid sealed inside each heat pipe and the energy takes place in four steps [7]. These are:

1. The fluid evaporates by solar radiation.
2. The vapor rises to the top, and when it meets a colder pipe, where a liquid flows through.

3. The vapor is condensed as transferring the latent heat to the liquid in the top pipe.

4. The condensed fluid in the tubes runs back to the bottom, where the process can start again.

ETCs have demonstrated that the combination of a selective surface and an effective convection suppressor can result in good performance at high temperatures. The vacuum envelope reduces convection and conduction losses, so the collectors can operate at higher temperatures than flat-plate collectors. Like flat-plate collectors, they collect both direct and diffuse radiation. However, their efficiency is higher at low incidence angles. This effect tends to give evacuated tube collectors an advantage over flat-plate collectors in terms of daylong performance [8].

Because no evaporation or condensation above the phase-change temperature is possible, the heat pipe offers inherent protection from freezing and overheating. This self-limiting temperature control is a unique feature of the evacuated heat pipe collector.

The thermal efficiency of ETC depends on many factors like material type of absorber, heat pipe, surface area and so on. The entire system is shown in Figure 7.

Solar Selective Surface

The most important and critical part of the collector is the absorber surface. Spectral selective solar absorbers increase the useful energy output [6]. The blackbody spectrum at a given temperature and the spectral distribution of the sun needed to be known in order to evaluate absorbing surface behavior. The standard spectral solar flux incident at the surface of the earth, after atmospheric absorption, is limited to the range between 0.3 and 2.5 μm i.e. UV/Vis/NIR wavelength ranges [12].

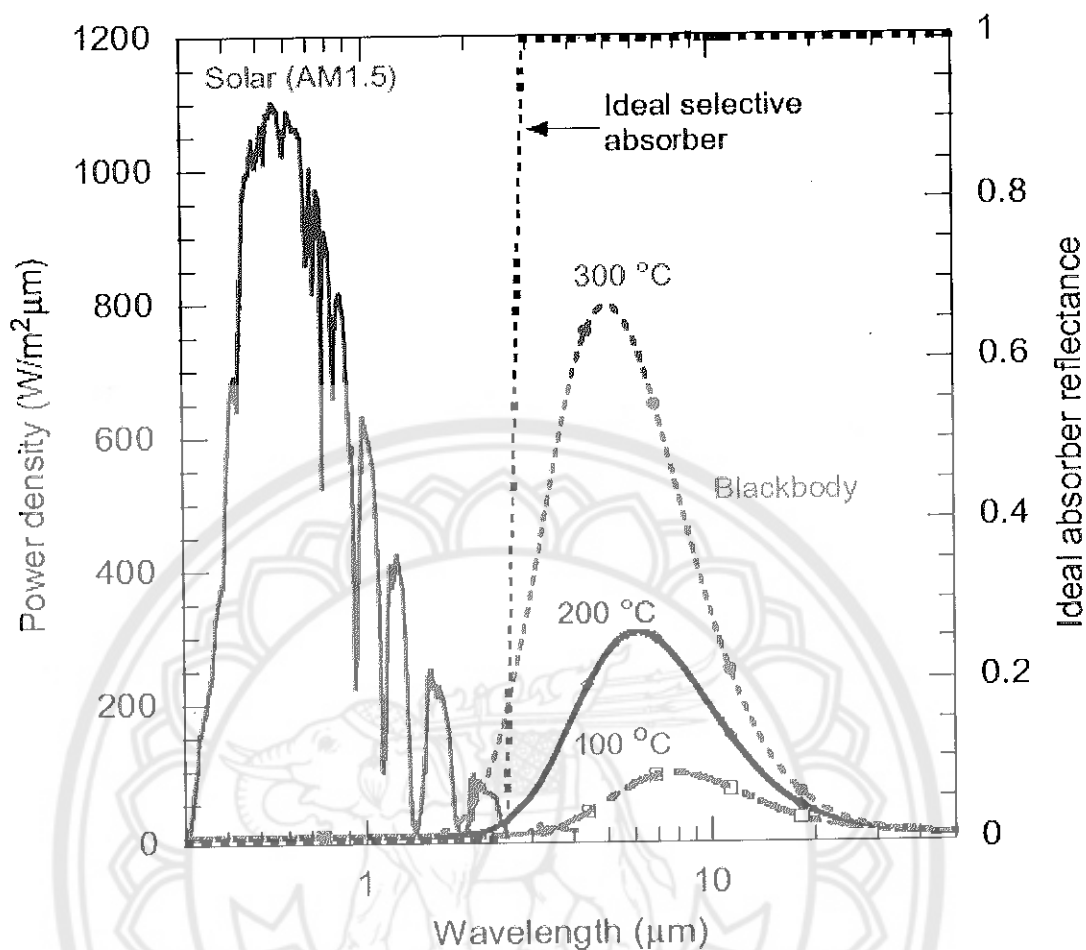


Figure 5 Solar spectral irradiance for AM^{1.5}. [13]

The above shows an annotation showing minimal overlap between the sun spectrum at AM^{1.5} and the black body like emission spectra at 100, 200 and 300°C. A reflectance curve for an ideal selective solar absorber is included. The blackbody spectrum for temperatures between 50° to 100°C and the solar spectrum do not overlap in any wavelength range, as shown in Figure 5. Therefore, it is possible to design a solar absorber plate surface which absorbs the maximum possible of the incident solar radiation, but does not re-emit the absorbed energy. A material having high absorptance (low reflectance) in the solar spectrum and low emittance (high reflectance) in the thermal infrared is called a selective solar absorber. An ideal spectrally selective surface should have a reflectance of zero in the solar wavelength range and unity in the thermal infrared. For temperatures below 100°C the on-set wavelength for the low to high reflectance is about 3 μm and for higher temperatures

($\approx 300^\circ\text{C}$) the critical wavelength is around $2\text{ }\mu\text{m}$. The solar absorptance is one parameter that characterizes the performance of the absorber. It is defined as the fraction of incident radiation at a given wavelength that is absorbed. For an opaque material the spectral absorptance can be expressed in terms of the total reflectance:

$$\alpha = \frac{\int_{\lambda_1}^{\lambda_2} (1 - R(\lambda)) I_s(\lambda) d\lambda}{\int_{\lambda_1}^{\lambda_2} I_s(\lambda) d\lambda} \quad (1)$$

The most common absorber type is the absorber-reflector tandem which is obtained by combining two surfaces, one surface which is highly absorbing in the solar region and another highly reflecting in the infrared. An alternative way to achieve the absorber-reflector tandem is to cover a thick absorbing surface by a solar transparent infrared reflecting coating which is normally called a heat mirror [6].

Commercial solar absorbers are made by electroplating, anodization, evaporation, sputtering and applying solar selective paints [7]. Aluminum has higher reflectivity but to use as solar absorber material, solar selective paint is required, in order to increase its solar absorptivity in solar spectrum region.

Coating

Oxide and sulfide layers were the first selective surfaces used in copper-based solar thermal systems. In the solar thermal industry semiconductor or metal tandems are used for selective absorption in the solar spectrum. Some inorganic compounds or metal/dielectric composites can be used as coatings for various applications, black chrome ($\text{Cr-Cr}_2\text{O}_3$) and black nickel (Ni-Zn-S) are the inorganic materials used in the solar thermal industry. Selective coatings can be applied to a surface using a large number of techniques. Generally, a coated surface for solar thermal application must fulfill the following points:

1. high absorptance in the solar spectrum and low emittance in the thermal spectrum,
2. the coating must adhere close to the substrate surface.
3. the coating should be stable under long thermal cyclic load.

4. the coating should be economical to apply.

Electroplating, chemical conversion, spray pyrolysis, vacuum deposition, and chemical vapor deposition are some of common coating techniques [14].

Painting

Paint is a combination of pigment, resin, solvent and additives. Pigments are tiny insoluble particles included into the paint mainly to contribute color by absorption and reflection of light[15]. Resins are binder to hold the pigment particles together and provide adhesion to the surface painted. Solvent acts as a carrier for pigments and resin. Additives are added to get desired features. Paint has some attractive features such as ease of processing, low cost, ease of field maintenance, and commercial availability. Paints can be applied by simple techniques such as roll coating (coil coating), dip coating, spin coating, spray coating and brush coating [14].

Their optical performance is governed by intrinsic optical constants as well as particle size-dependent scattering and absorption. The combined effect gives the effective scattering and absorption coefficients of the pigment particles. Polymers such as silicone, siloxane resin or phenoxy resin are usually used as binders. Unfortunately, binders in general absorb infrared radiation and thereby the thermal emittance is higher. The particles usually agglomerate and their size becomes comparable to or larger than the incident wavelength of light. In order to reduce the agglomeration, fumed silica can be added during the preparation of the paints. Laboratory studies of a range of pigments (mostly metal oxides) on aluminum substrates have been reported and the best obtained result was for an iron-manganese-copper oxide (FeMnCuO_x) pigment with a silicone binder, giving a solar absorptance of 0.92 and a thermal emittance of 0.13. Thickness sensitive spectrally selective (TSSS) paints obtained from FeMnCuO_x in a siloxane resin matrix have good optical properties ($\alpha = 0.90 - 0.92$ and $\varepsilon = 0.20 - 0.25$) [6].

Thermal Performance

The thermal efficiency is the ratio of energy collected to the total solar energy. The thermal equation of solar collector under steady state conditions, is described in Kalogirou 2009 as follows [7]:

The useful energy gain from the collector is calculated as mentioned in equation 1 and the efficiency is calculated as the ratio of useful energy to input energy.

$$Q_u = \dot{m}c_p(T_o - T_i) \quad (2)$$

$$\eta = \frac{\dot{m}c_p(T_o - T_i)}{A_a G_i} \quad (3)$$

The heat removal factor F_R is defined as the ratio of actual useful energy output that would result if the collector surface is at the local fluid inlet temperature. And considering the optical parameters and overall heat transfer coefficient, the useful energy collected from a solar collector will be:

$$Q_u = A_a F_R [G_i (\tau\alpha)_n - U_L (T_i - T_a)] \quad (4)$$

The thermal efficiency is obtained by dividing the useful energy by the energy input ($A_a G_i$):

$$\eta = F_R (\tau\alpha)_n - F_R U_L \left(\frac{T_i - T_a}{G_i} \right) \quad (5)$$

For collector operating under steady irradiation and fluid flow rate, the factors $F_R (\tau\alpha)_n$ and U_L are nearly constant. So equation no. (3) will be a straight line equation, its slope will be equal to $-F_R U_L$ (which is the efficiency difference divided by the corresponding horizontal scale difference), it is shown in Figure 7.

The intercept (intersection of the line with the vertical efficiency axis) equals to $F_R (\tau\alpha)_n$. If the collector heat delivery at various different temperatures and solar conditions are plotted with efficiency as the vertical axis and $\frac{\Delta T}{G_i} = \frac{(T_i - T_a)}{G_i}$ as the

horizontal axis, the best straight line through the data points correlates the collector performance with solar and temperature conditions. When temperature of inlet equals the ambient temperature, collector efficiency will be maximum and equals to $F_R (\tau\alpha)_n$.

At the intersection of the line with horizontal axis, collector efficiency is zero, it corresponds to low radiation level/ high temperature of the fluid into the collector (heat losses equal to solar absorption and called Stagnation).

The maximum temperature is given by:

$$T_{\max} = \frac{G_i(\tau\alpha)_n}{U_L} + T_a \quad (6)$$

In reality the heat loss coefficient U_L is not constant but it is a function of the collector inlet and ambient temperatures.

$$F_R U_L = c_1 + c_2(T_i - T_a) \quad (7)$$

Substituting the above equation in to eq 4:

$$Q_u = A_a F_R \left[(\tau\alpha)_n G_i - c_1(T_i - T_a) - c_2(T_i - T_a)^2 \right] \quad (8)$$

Therefore, thermal efficiency can be generalized as:

$$\eta = F_R(\tau\alpha)_n - c_1 \frac{(T_i - T_a)}{G_i} - c_2 \frac{(T_i - T_a)^2}{G_i} \quad (9)$$

if $c_0 = F_R(\tau\alpha)_n$ and $x = \frac{(T_i - T_a)}{G_i}$ then

$$\eta = c_0 - c_1 x - c_2 G_i x^2 \quad (10)$$

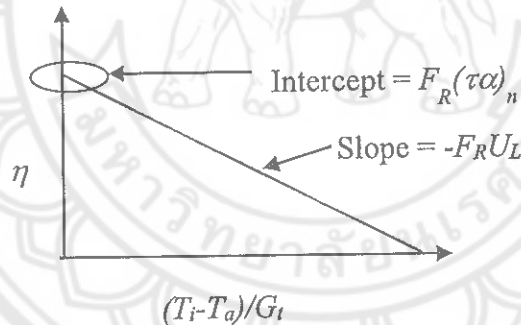


Figure 6 Performance curve of ETC

Figure 7 shows the system circuit according to the ISO 9806-1 standard.

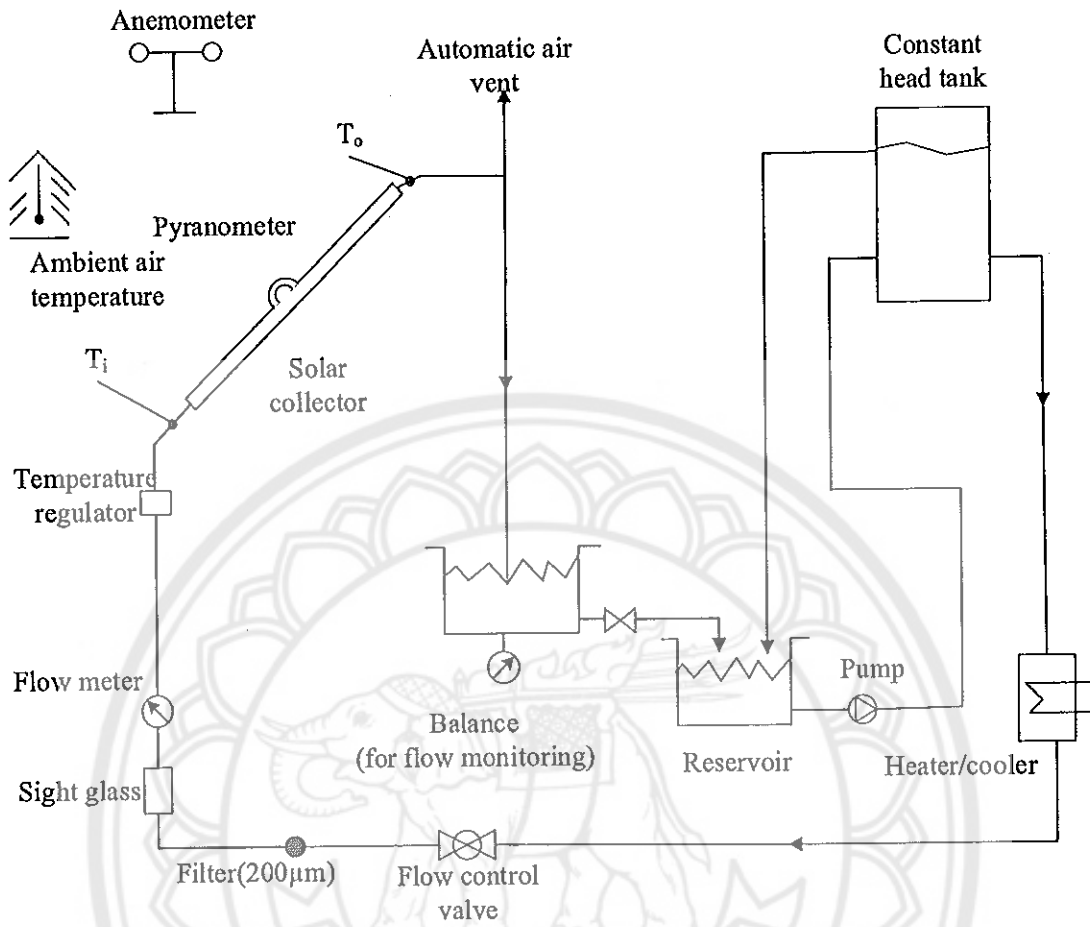


Figure 7 Open loop test system [7]

Economical Evaluation

LCOE is an important parameter of economic analysis, and considers initial capital cost, operating cost, energy produced each year, interest rate, project period and year at the end of the project. The initial cost includes the cost of the ECT, paint and painting process. Normally the operating cost and salvage cost is assumed to be 0.5% and 10% of initial cost respectively.

$$LCOE = \frac{C_c + \sum_{n=1}^N \frac{C_n}{(1+i)^n}}{\sum_{n=1}^N \frac{E_n}{(1+i)^n}} \quad (10)$$

Literature Review

Hazami, M. et al. [16] studied experimentally and using TRNSYS simulation program to determine the energy performance of ETC and FPC used for domestic solar water heater (DSWH) installed in Tunisia and found that the solar fraction to be 84% and 68% for ETC and FPC respectively and also found ETC can generate 9% more energy than FPC.

Gao, Y. et al. [17] did experiment on thermal mass and flow rate influence on forced circulation solar hot water system using the water in glass evacuated tube solar collector (WGETC) and U-pipe evacuated tube solar collector (UpETC). Due to thermal mass influence for flow rate 10-70 kg/h·m², the WGETC storage energy is 25%-35% less than that of Up ETC.

Ayompe, & Duffy [18] analyzed thermal performance of solar water heating system ETC in Dublin, Ireland. And found annual average daily energy collected was 20.4 MJ/d and energy delivered by solar coil was 16.8 MJ/d. The solar fraction was 33.8%, collector efficiency was 63.2% and system efficiency was 52%, suggested the length supply pipe should be as short as possible to decrease the heat loss from the supply pipe (which covered 17.7% of the energy collected).

Ma, L. et al. [11] studied analytically on thermal performance analysis of the glass evacuated tube solar collector with U-tube and found the influence of thermal resistance of air layer (between the heat pipe and the inside part of the glass tube) on heat efficiency is large. Efficiency of solar collector increases 10% and the outlet fluid temperature increase by 16% if the synthetically conductance increases from 5 to 40W/m.K and coating temperature will increase to 30°C if the thermal resistance of the air layer is taken in to account. In general, the heat losses reduced and heat extraction was high.

Yamaguchi, H. et al. [19] proposed and experimentally studied using the supercritical carbon dioxide (R744 CO₂) as working fluid in the solar water heater using ETC. The result from the experiment shows that natural convective flow is well induced and a flow of 1900 Reynolds number can achieved even in winter, the collector and heat recovery efficiency 66% and 65% are measured respectively.

Morrison, G.L. et al. [10] showed that the water in glass evacuated tube solar water heater operates effectively in a range of climatic conditions.

Morrison, G.L. et al. [20] the storage tank temperature and the intensity of the radiation which fall on to the absorber surface influence the circulation flow rate through the tubes, and the circulation rate is strongly influenced by the inlet conditions of the tube.

Jyothi, J. et al. [3] design and fabricated a tandem absorber type, which is TiAlC/TiAlCN/TiAlSiCN/TiAlSiCO/TiAlSiO, on stainless steel substrate, the first three layers in this tandem act as an absorbing layer, whereas, TiAlSiCO and TiAlSiO act as semi-transparent and anti-reflecting layers and found absorptance of 0.961 and emittance of 0.07 at 82°C.

Orel et al. [21], applied paints on aluminum, copper and stainless steel foils and found that the method of application of paint strongly influences the final spectral selectivity. And better results were obtained when the paint was applied by draw bar coater due to more homogeneous distribution of the applied paint over the substrate.

Tesfamichael, T. [6] reported the solar absorptance is one parameter that characterizes the performance of the absorber and for opaque material the spectral absorptance can be expressed in terms of the total reflectance, $R(\lambda, \theta)$. From his laboratory studies a range of pigments on aluminum substrates have been reported on iron-manganese-copper oxide (FeMnCuO_x) pigment with silicone binder, giving solar absorptance of 0.92 and thermal emittance of 0.13. And thickness sensitive spectrally selective (TSSS) paints obtained from FeMnCuO_x in a silicone resin matrix has ($\alpha = 0.90 - 0.92$ and $\varepsilon = 0.20 - 0.25$).

Gunde et al. [22], different coarse pigment size of the same paint composition was applied on aluminum foil by coil coating and spraying techniques to know the influence on the solar absorptance. They found that in solar spectral range the absorption coefficient is diminished with particle size for sprayed layers whereas coil coated films appear to be unaffected.

Kunic, R. et al. [23] studied thermal degradation of the TSSS PU B ($\alpha = 0.90$, $\varepsilon = 0.20$), and TISS PU A coatings ($\alpha = 0.90$, $\varepsilon = 0.38$), both of them are polyurethane resin binder. And find binder B is more stable than Binder A.

Orel, B. et al. [24] Low emittance is attained by the addition of bare aluminum, colored aluminum flake pigments or copper flake pigments, while other inorganic pigments impart various colors to the paints. Moreover, the dispersed

pigments in silicone resin binder imparting the TISS paint coatings high-temperature tolerance, excellent adhesion, UV resistance, flexibility and weather-durability, which make them suitable coatings for colored glazed or unglazed solar absorbers.

Lundh, M. et al. [25] studied that solar absorptance of two commercial TSSS paints can be increased between 0.01 and 0.02 units with antireflection treatment using silicone dioxide layer deposited from silica gel.

Orel B. et al. [26] used Polyurethane resin for preparing the red, green, and blue paints for use as (TISS) paint coatings for solar façade absorbers.

Orel, & Gunde [27] studied the important parameters for designing spectrally selective paint coatings. By changing the compositions of paints, additional optical properties of coating can be achieved. Moreover, type of pigment used for paint preparation was defined. And confirms adding more black pigment does not mean always to increase the absorption.

Therefore, presently the solar paint, ThurmaloX 250 selective black solar collector coating, was applied on different thicknesses of Al fin with spray deposition technique in order to study the effects of Al fin thicknesses on the thermal efficiencies of ETC. Moreover, the optical characterization of solar paint coated Al fin having different coating thicknesses was studied.

Table 2 Summary of the Literature Review

Author	Type of investigation	Description of the test	Findings
Hazami et al. (2013) [16]	Experimental	Water as working fluid in ETC	ETC DSWH (84%) has higher solar fraction (i.e. in average) than FPC DSWH (68%) annually. And ETC can generate approximately 9 % more energy than FPC.
Geo et al. (2013) [17]	Experimental	Antifreeze fluid (40% glycol by volume) in WGETC and UPETC	In average, the thermal efficiency of WGETC is less than UPETC.
Ayompe and Duffey (2013) [18]	Analytical	Water as working fluid in HP-ETC	Comparing UPETC and WGETC with the same efficiency curves, WGETC achieves energy storage of 25–35% less than UPETC.
Ma et al. (2010) [11]	Analytical	Water as working fluid in Glass evacuated tube (with U shaped absorber tube)	To operate solar water heating system, HP-ETCs are more efficient than their FPCs. Outlet temperature 38 °C, efficiency 59%, collector efficiency increases with in synthetic conductance. Heat losses reduced and Heat extraction is high. The challenge is to preserve vacuum environment.
Yamaguchi et al. (2010) [19]	Experimental	R744CO ₂ as working fluid in UPETSC	Collector efficiency 66% Heat recovery = 65%

Table 2 (cont.)

Author	Type of investigation	Description of the test	Findings
Morrison et al., (2004) [10]	Numerical	Water in glass	operates effectively in a range of climatic conditions
Morrison et al. (2005) [20]	Experimental and numerical simulation	Water as working fluid in WGETSC	Storage tank temperature and the intensity of the radiation which fall on to the absorber surface influence the circulation flow rate through the tubes. Circulation rate is strongly influenced by the inlet conditions of the tube.
J.Jsyothi (2015) [3]	Experimental	Spectrally selective surface deposited on stainless still substrate	$\alpha = 0.961$ and $\varepsilon = 0.07$ at 82°C
Orel, et al. (2001) [21]	Experimental	Techniques of paint application on substrate	Affects the final solar selectivity draw bar coater is better than the other method.
Tuquabo	Experimental	Characterization of FeMnCuO _x	FeMnCuO _x with silicone binder ($\alpha = 0.92$ and thermal $\varepsilon = 0.13$)
Tesfamicheal (2000) [6]			FeMnCuO _x with silicone resin ($\alpha = 0.90$ - 0.92 and thermal $\varepsilon = 0.20$ - 0.25)

Table 2 (cont.)

Author	Type of investigation	Description of the test	Findings
Gunde, et al. (2003) [22]	Experimental	Different pigment size applied on aluminum foil	In solar spectral region the abs. coefficient decreases with particle size of the sprayed layers.
R. Kunic 2011 [23]	Experimental	Thermal degradation on solar selective surfaces	Binder B (TSSS pu B) is more stable than Binder A (TISS Pu A)
Orel,B. et al. (2007) [24]	Experimental	TISS Paints	Low emittance is attained by addition of bare aluminum excellent adhesion, UV resistant, flexibility and weather durability
Lundh, M., etal (2010) [25]	Experimental	Antireflection treatment on TSSS Paints	Absorptance can be increased from 0.01 and 0.02 with antireflection treatment.
Orel B., et al. (2007) [26]	Experimental	Preparation of TISS using Polyurethane as resin	prepared red, green, and blue colored paints for solar facade absorbers.
Orel and Gunde (2000) [27]	Experimental	parameters for designing spectrally selective paint coatings	by changing the compositions of paints, additional optical properties can be achieved identified the type of pigment used in paint

Table 2 (cont.)

Author	Type of investigation	Description of the test	Findings
Presently study	Experimental	Experimental on ETC by coating different thickness of Al fin with solar paint	The effect of various aluminum fin thicknesses coated with solar paint absorber thickness on thermal performance will be studied

CHAPTER III

RESEARCH METHODOLOGY

Research Area

The experiment is carried out in the School of Renewable Energy Technology, Naresuan University (16.47°N latitude and 100.16°E longitude), Phitsanulok, Thailand.

Equipment and Material Used

Coating of Al with solar paint

Before the application of paint on Al, the surface was cleaned with acetone in order to remove foreign particles from the surface. Gloves were used in order to avoid any mark created from our hand. A spray gun with its compressor is used for the application of the solar paint (spray deposition method) on Al fin absorber. Aluminum material is designated as AA6061 and its composition is explained in the table below.

Table 3 composition of Al [28]

Component	Wt. %	Component	Wt. %	Component	Wt. %
Al	95.8 - 98.6	Mg	0.8 - 1.2	Si	0.4 - 0.8
Cr	0.04 - 0.35	Mn	Max 0.15	Ti	Max 0.15
Cu	0.15 - 0.4	Other, each	Max 0.05	Zn	Max 0.25
Fe	Max 0.7	Other, total	Max 0.15		

Selective solar collector paint, ThurmaloX 250 selective black solar collector coating, Damaney Company, Inc USA, will be applied by spray deposition technique (using spray gun operated with air compressor) on aluminum sample with variety of coating thickness. Appropriate solar paint thickness will be selected based on better solar spectral selectivity of the samples which is determined from the characterization study.

The choice of thinner will influence the coating's average selective characteristics. For optimum selectivity, slow-evaporating thinner such as Dampney 100 with 1:1 ratio is used (Dampney Company, Inc.). The solar paint will be applied on the three different aluminum fin absorber thickness. The cross section of the evacuated glass tube with aluminum fin absorber is shown in the Figure 8.

Table 4 Properties of Thurmalox 250 black solar paint [29]

Description	Remark
Selective surface	
Resists outgassing to 204°C	
Heat resistant to 538°C	
Resistant to UV degradation	
Solar Absorptivity $\alpha = 0.96$	With 1:1 mixing ratio
Emissivity $\varepsilon = 0.52$ to 0.80	With 1:1 mixing ratio
Dries for handling in 30 minutes	
Air dry or heat cure	

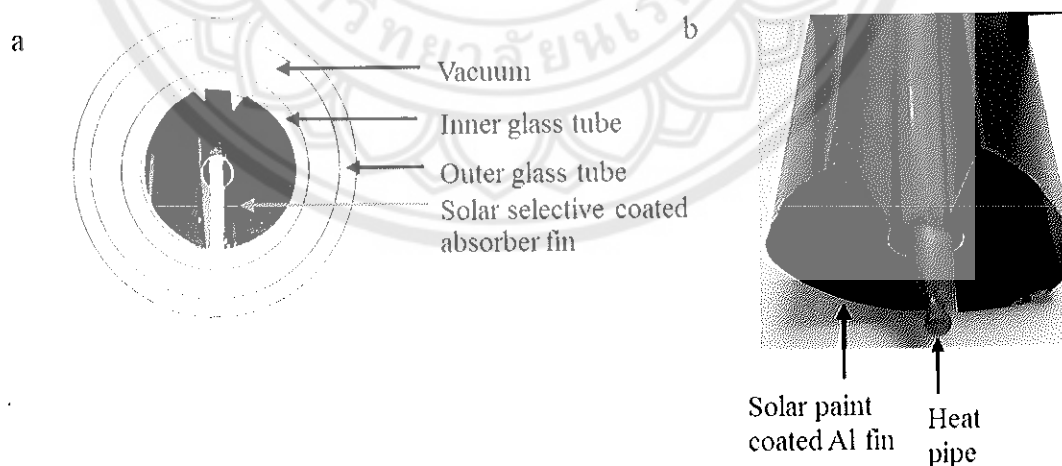


Figure 8 a) Cross section of new coating b) Coating on Al fin solar absorber

Characterization of samples

Below listed are the materials used for characterization of Al fin sample and determining the thermal performance of the ETC.

For characterization, the following equipment are used:

1. Electro Physic MiniTest- 730 (model 730, nondestructive coating thickness measurement, Germany) for measuring the coating thickness.



Figure 9 Digital mini Test 730

Source: <http://www.obsnap.com>

2. X-ray Diffractometer (XRD Rigaku miniflex II X-ray diffraction) was used for determining the phase of the coated Al fin surface.

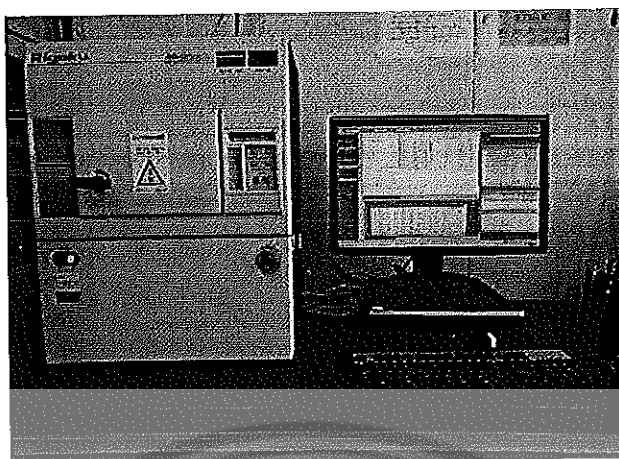


Figure 10 Rigaku miniflex II X-ray diffraction

Source: <http://scs.kyushu-u.ac.jp/kan/en/images/content/07.jpg>

3. Ultraviolet-Visible-Near Infrared Spectrophotometer (UV-Vis NIR Spectrophotometer) used for measuring the reflectance of the painted surface in the wavelength range of 300 to 2500 nm.

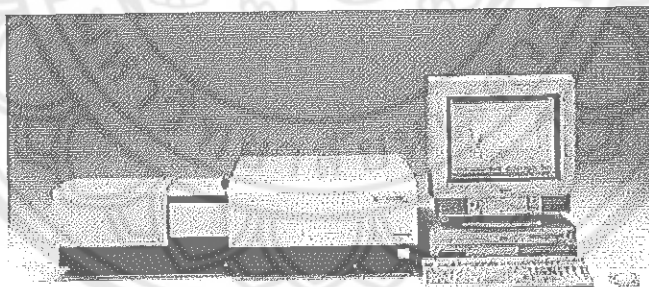


Figure 11 Ultraviolet-Visible-Near Infrared Spectrophotometer

Source: <http://www.speciation.net/Database/Instruments/Shimadzu-Europe/UV3101>
PC-;i1302

For determining the thermal efficiency of the ETC, an outdoor testing of ETC system was done. The protocol of the testing was done according ISO 9806-1

standard. Three aluminum absorber fins which are available in the market with different thicknesses were considered.

1. Sheet No.1 with thickness of 0.11mm
2. Sheet No.2 with thickness of 0.13 mm
3. Sheet No.3 with thickness of 0.24 mm

Table 5. Collector specification

Collector specification	Description and measurement
Size (length x width x height)	1.8 x 1.1 x 0.14 meters
Gross area	1.98 m ²
Absorber area	1.08 m ²
Working fluid	water
Absorber material	Aluminum (AA6061)

The transmissivity (τ) of Borosilicate glass is taken $\tau = 0.91$ [30].

An ETC with the above specification were mounted on collector testing ring that have robot motor that enables to track sun consciously. The working fluid is water. The Aluminum sheets will have the same coating type and coating thickness. RTD sensors were used to read the inlet and the outlet temperature and calibrated pv reference cell was used for measuring the total irradiance (direct beam plus diffuse). All the necessary data were recorded using the Agilent data Logger which is connected with the system and computer.

Outdoor Testing of ETC and Experiment Condition

The following conditions will be taken during the experiment. One experiment for each Al fin solar absorber thickness was done. The experiment follow the ISO 9806-1 standards [31]. Open loop type was used in the experiment, as shown in figure 10. Certain parameters held constant with some given tolerance to fulfill the requirement as the experiment follow the steady state test. And these are:

1. Solar radiation greater than 800W/m².
2. Wind speed must be maintained between 2 and 4m/s.

3. Angle of incidence of direct radiation is within $\pm 2\%$ of the normal incident angle.

4. Fluid flow rate should be set at 0.02 kg/s m^2 .

Table 6 tolerance of measured parameters

Parameters	
Test solar irradiance	$\pm 50 \text{ W/m}^2$
Surrounding air temperature	$\pm 1 \text{ K}$
Fluid mass flow rate	$\pm 1 \%$
Fluid temperature at the collector inlet	$\pm 0.1 \text{ K}$

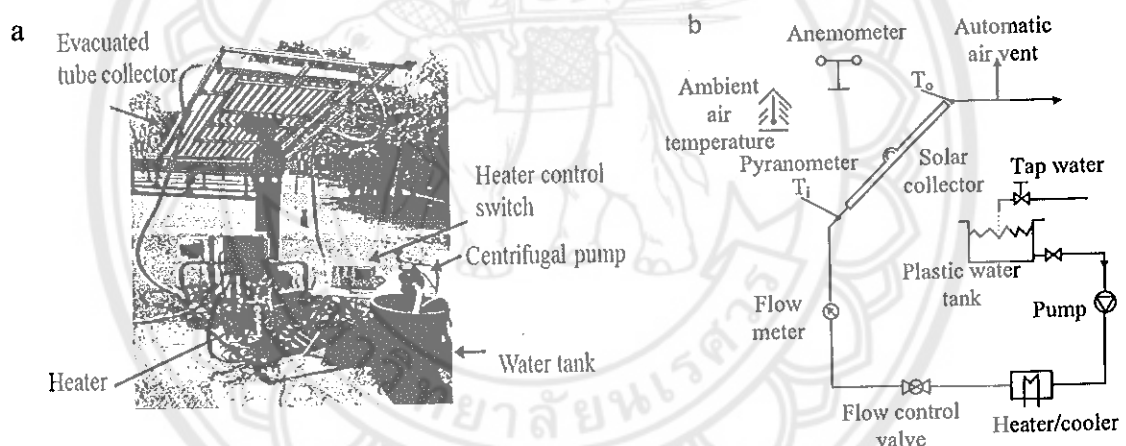


Figure 12 (a) Equipment setup and (b) its equivalent schematic diagram

For the tests, the following parameters were needed to be measured:

1. Global solar irradiance at the collector plane, G_T
2. Air speed above the collector aperture
3. Ambient air temperature, T_a
4. Fluid temperature at the collector inlet, T_i
5. Fluid temperature at the collector outlet, T_o
6. Fluid flow rate, \dot{m}

Calculation and Analysis

1. Solar Absorbance (α)

After the reflectance result from the UV-Vis near infrared test, the absorbance was calculated using equation 1 [32].

2. Thermal Performance evaluation

From pervious publication [7] the steps for computing the thermal efficiency and other parameters are as follows:

2.1 Using the data recorded from the experiment like mass flow rate, inlet and outlet water temperature the thermal efficiency will be determined at various in let fluid temperature using equation 3.

2.2 The performance curve, efficiency verses ratio of temperature gradient to global irradiance will be drawn and the best curve fitting will be found using linear regression method as shown in Figure 6.

2.3 Compare the equation of the curve with the general thermal efficiency formula (equation 10) to find the coefficients.

After calculating the efficiencies of all the three ETC with different aluminum sheet thickness, efficiency vs ratio of temperature gradient to global solar insolation is drawn.

Levelized cost of energy (LCOE)

Levelized Cost of Energy, LCOE will be calculated using equation 10, which considers initial capital cost, operating cost, energy produced each year, interest rate, project period and year at the end of the project.

The cost analysis included the three different al fin thickness ECT. The components of LCOE is shown in figure 13. And the initial investment and setup costs includes:

1. Cost of the Al fin solar absorber
2. Cost of the solar paint and painting process
3. Cost of the ECT testing ring.

Based on the outcomes of technical performance and evaluation of LCOE of each thickness of Al fin absorber, comparison will be done among the three ETC with

different aluminum fin thickness and also with the commercial available ETC in the market.

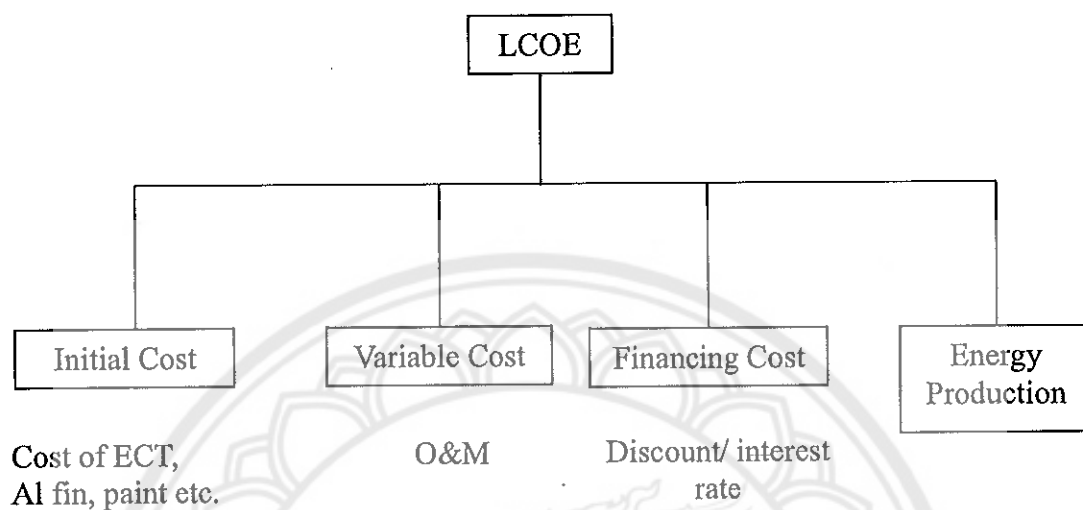


Figure 13 Components of LCOE

Procedure and methodology

The procedure and methodology in this study looks as shown in figure below.

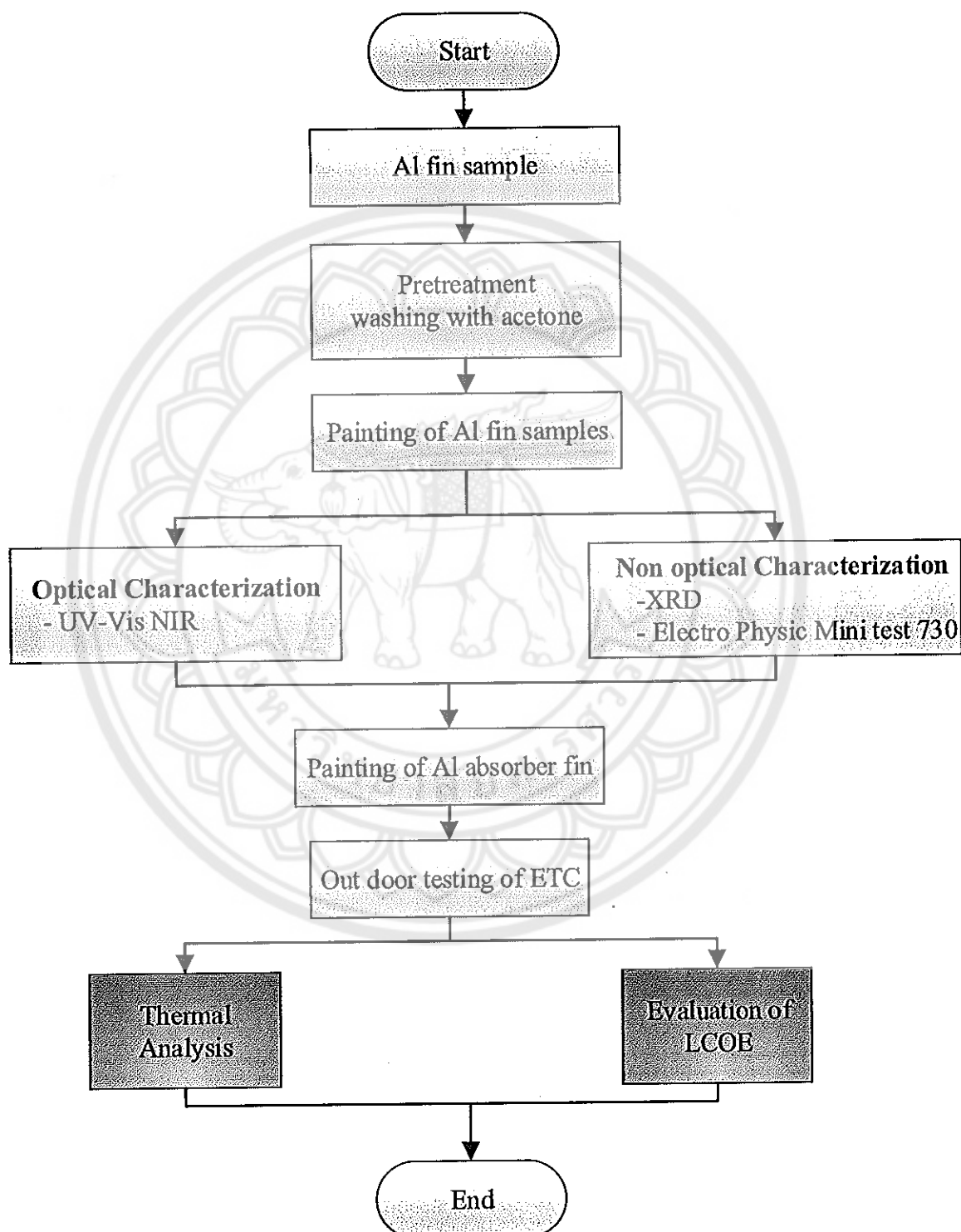


Figure 14 Flow Chart of Procedure and methodology of the study

CHAPTER IV

RESULT AND DISCUSSION

As stated in the methodology, after the preparation of three sample with single, double and triple layer of coating, the samples were taken for the characterization of reflectance and identification of coating thickness.

The coated Al was drying and were used after one day in order to make sure that completely dried.

Determination of coating thicknesses

A digital device called Mini Test 730 was used to determine the thickness of coating. At different 50 positions of a sample was measured and then average was taken. The result is shown in Table 17-19.

The histogram curve for the coating thicknesses are as follows:

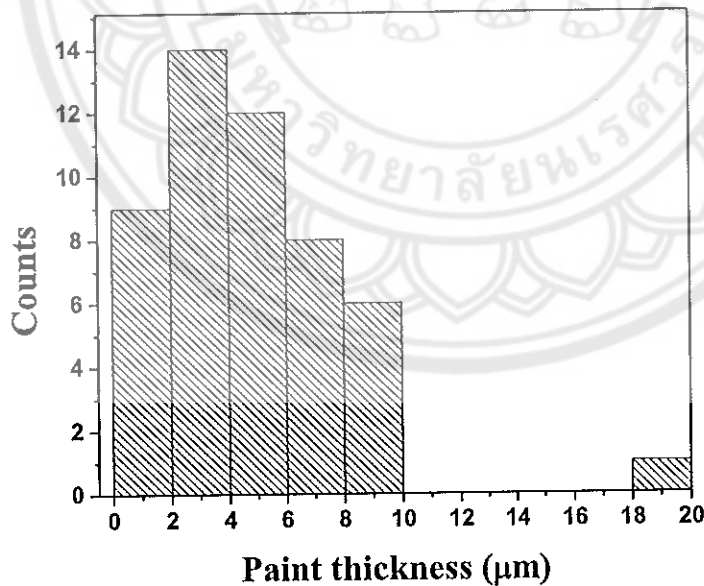


Figure 15 Histogram curve of solar paint thickness for single layer coating

The painting thickness for the first single layer (1x) looks as shown in the Figure 15, with average coating thickness of $4.76\text{ }\mu\text{m}$. The thickness distribution was bounded mostly between 0.25 to $9.95\text{ }\mu\text{m}$ except in one point scores $19.30\text{ }\mu\text{m}$. For second layer coating (2x) shown in figure 16, recorded an average value of $5.88\text{ }\mu\text{m}$. The triple layer coating (3x) got an average thickness of $11.174\text{ }\mu\text{m}$, and the distribution looks more uniform (Figure 17) compared to the others.

The 1x and 2x layer coating are in good agreement with the manufacturing specification (1.5 to $6.4\text{ }\mu\text{m}$) but the third one is an insignificantly higher [29]. However, all of the solar paint thicknesses are too low comparing with Solkote commercial selective solar coating thickness (20 to $25\text{ }\mu\text{m}$) [33].

It was observed that the number of layer coating got linear relation with the coating thickness and these makes the spray deposition technique weak compared to the other method like draw bar coating, where the painting and pigment distribution is uniform.

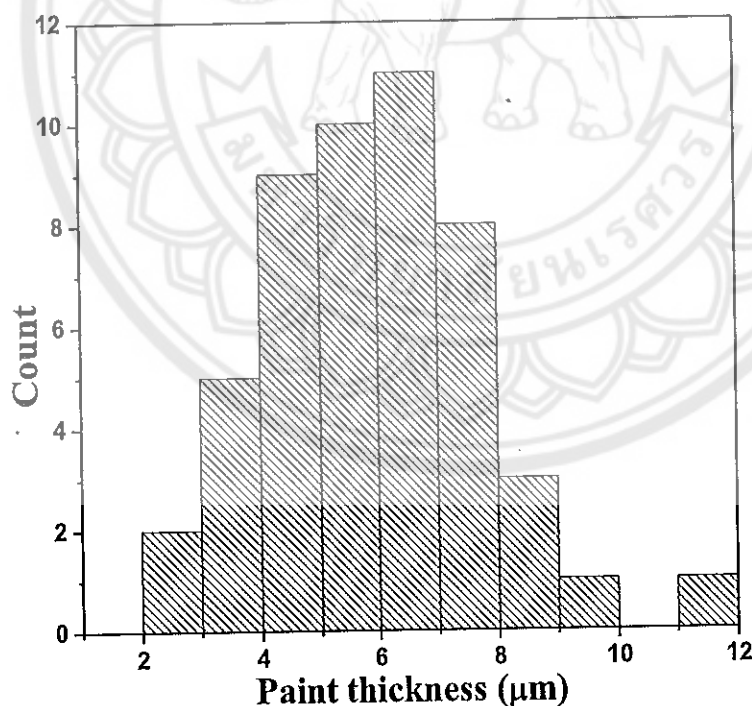


Figure 16 Histogram curve of solar paint thickness for double layer coating

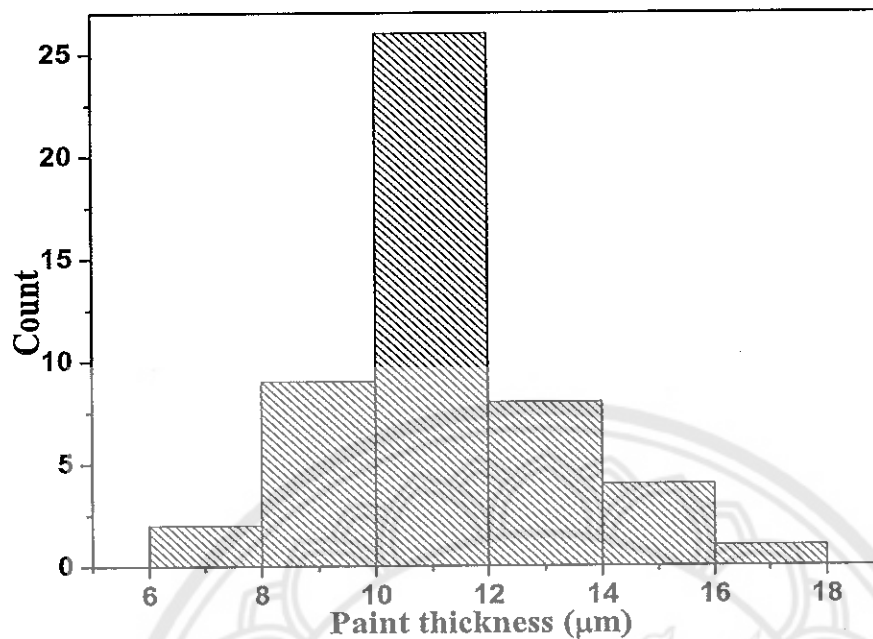


Figure 17 Histogram curve of solar paint thickness for triple layer coating

From the above data, it could be understood that there is significant difference of thickness of painting among the three different layers. The first two are in good agreement with the manufacturing specification (1.5 to 6.4 μm) but the third one is a little bit higher [29]. And all are too low comparing with Solkote commercial selective solar coating thickness (20 to 25 μm) [33].

Ultraviolet- Visible- Near Spectrometer analysis

Figure 18 shows the measured reflectance and calculated solar absorptance at each wavelength of (R) and (α) respectively and spectra of the solar painted Al absorber, together with the sun spectrum at AM 1.5 in the wavelength interval 300-2500 nm of solar painted Al at thickness of 4.76, 5.88, 11.174 μm . The absorptance and reflectance values of painted Al absorber are listed in Table 7.

Table 7 R and α of the three different painting thickness

Thickness (μm)	Average Reflectance	Average Solar Absorptance
4.76	0.06	0.9396
5.88	0.06	0.9366
11.174	0.06	0.9414

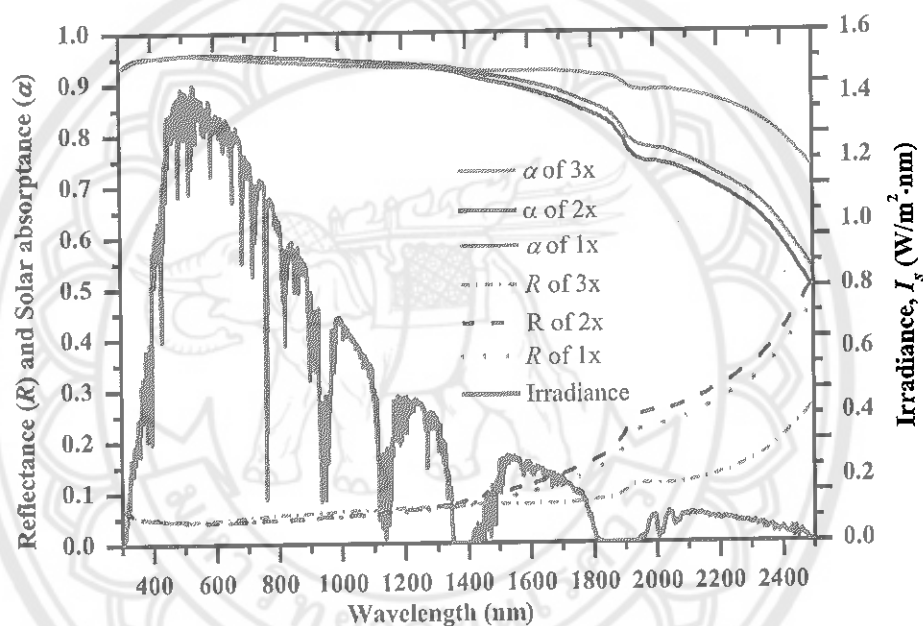


Figure 18 Spectral reflectance (R) and solar absorptance (α) curves of coated Al solar absorber comparing with the sun spectrum at AM 1.5 in the wavelength interval 300–2500 nm for single (1x), double (2x) and triple (3x) layer coated Al absorber fin.

According to the experimental results, the α of the three different paint thicknesses are similar values. This reveals that solar absorptance does not have much differences along the paint thicknesses considered (4.76 to 11.17 μm). As the result, all the real Al fin absorber is painted with single layer of solar paint. When the α is compared to that of commercial solar paint, $\alpha=0.96$ [29], reduced by 2.1% but a bit

higher when it is compared with TiO_2 paint in silicone resin binder which has an α of 0.90 [14]. More or less the values are in good agreement with the other related paints.

X-ray Diffraction analysis

Figure 19 shows that the XRD pattern of the coated Al, Al fin/sheet, compared with the JCPDS database of Al and Al_2O_3 with the reference no. 004-0787 and 01-1243 respectively. In the diffraction pattern, majority of diffraction peaks from Al fin were observed, and some peaks were from Al_2O_3 . In the low value of diffraction angle two peaks were observed which comes from the pigment of the solar paint. The diffraction pattern reveals that the painted surface was dominated by the Al material, and these could suppress the function of the solar paint to some extent.

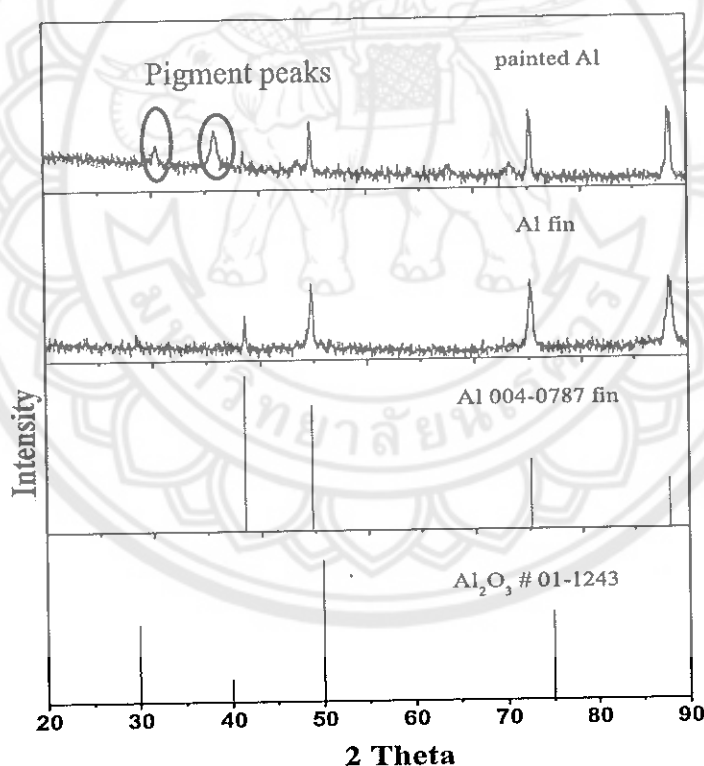


Figure 19 XRD pattern of solar paint coated Al and Al fin

Evaluation of thermal efficiency of the ETC

After the solar absorber fin is painted, it was inserted in the evacuated tube and assembled for carrying out the outdoor ETC performance test. During insertion the solar paint was observed to make scratches easily.

As shown in the graph below the η decreases as the inlet water temperature increases and this is mainly due to the increase of temperature gradient between the ambient the outlet water temperature which indirectly increases the heat loss to the surrounding. The decreasing rate is different for the three samples as the thickness is different which causes the U_L value to vary.

From the collected data, the η were calculated and the performance curve, η verses $(T_i - T_a)/G_t$ was drawn as shown in Fig. 20 for the three different Al fin absorber thicknesses. 55%, 50% and 38% of optical efficiency were recorded for ETC of 11, 13, 24 μm Al fin thickness respectively.

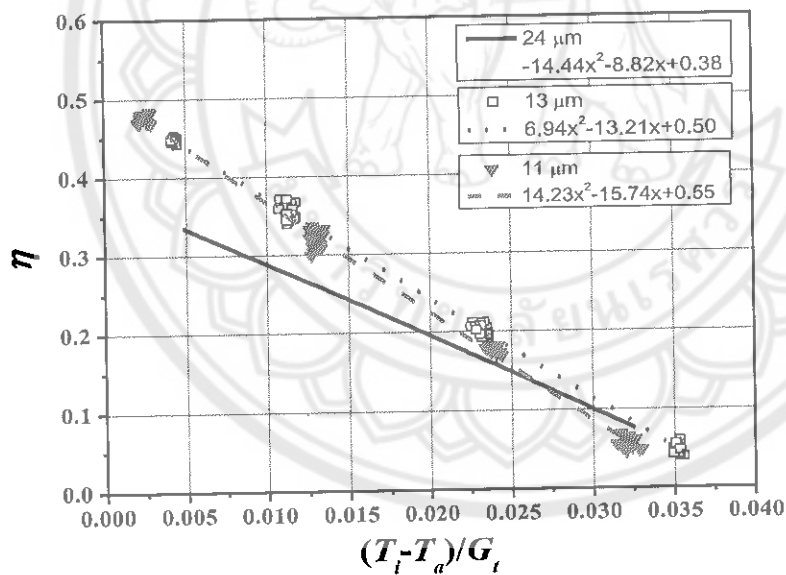
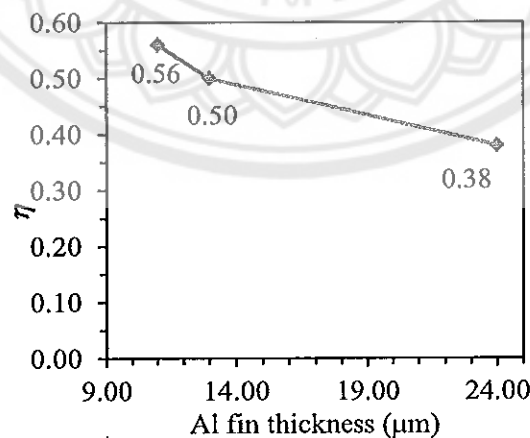


Figure 20 Comparison of performance curve of ETC using Al fin thickness of 11, 13 and 24 μm as the solar absorber

Table 8 General equation of ETC

$\eta = F_R - c_1 \frac{(T_i - T_a)}{G_i} - c_2 \frac{(T_i - T_a)^2}{G_i}$	Al fin (μm)	$c_0 =$ $F_R(\tau\alpha)_n$	F_R	U_L	$c_1 =$ $F_R U_L$	c_2
$0.5535 - 15.738x - 14.23x^2$	11	0.55	0.64	24.59	15.74	0.0158
$0.5045 - 13.205x - 6.9411x^2$	13	0.50	0.58	22.77	13.21	0.0077
$0.3782 - 8.815x - 14.435x^2$	24	0.38	0.44	19.94	8.82	0.0156

The 11 μm Al fin thickness has higher heat removal factor, heat loss coefficient and thermal efficiency. The heat removal factor increase by 45% as the Al absorber thickness decrease by 54%. Even though the heat loss coefficient increases by 13%, the change is dominated by the increase of heat removal factor that ends in increasing the efficiency. Addition of more Al fin thickness results in increasing heat transfer resistance. The decrease of Al fin thickness causes the heat transfer rate to increase across the Al cross section and this matches ideally with one dimensional heat transfer theory. When the 11 m Al fin ETC compares with the previous publication, the optical efficiency c_0 decrease by 29.1% due to the low value of FR, the first order coefficient c_1 increase by 76.4% and the $c_2 G_i$ decrease by 21.78% this is mainly due to the increase of heat loss coefficient in this study [16].

**Figure 21 η versus Al fin solar absorber thicknesses of the ETC curve**

Regarding the efficiency vs thickness trend, as shown in figure 21, the decrease in thickness causes the efficiency to increase. Any addition of Al thickness increases the heat transfer resistance that mean it decelerate the useful heat gain from the collector which indirectly decreases the thermal efficiency of the collector. Therefore, as long as the durability and material stability is guaranteed, thinner Al fin can be used as solar absorber and heat transfer material in the ETC application.

Comparing with the previous study made for flat plate and evacuated tube collector is as follows.

Table 9 Comparison of thermal efficiency equations [16, 34]

		Thermal efficiency equation
Present study	11	$\eta = 0.55 - 15.74x - 14.23x^2$
	13	$\eta = 0.50 - 13.21x - 6.94x^2$
	24	$\eta = 0.38 - 8.82x - 14.44x^2$
Hazami, M. et al		$\eta = 0.71 - 3.72x - 17.33x^2$
Company I (ETC)		$\eta = 0.57 - 0.54x - 2.88x^2$
Company J (ETC)		$\eta = 0.80 - 2.77x - 16x^2$
Company A (FPC)		$\eta = 0.57 - 21.91x$
Company B (FPC)		$\eta = 0.62 - 10.37x$

As mentioned the performance curve of various collector in table 9, the present study has lower efficiency. The maximum (optical) efficiency of the 11 m ETC is decreased by 29% and 45% compared to the solar collector tested by Hazami, M. et al and Company J respectively. But compared to others it decreases with slight percentage.

Generally, the general performance equation of current study has lower optical efficiency due to mainly the weak adhesive bonding of solar paint with Al fin substrate and some heat losses in the inlet and outlet pipe of ETC which has a total length of 6 meters.

Evaluation of LCOE for ETC using different Al fin thicknesses

An economic assessment of the use of different Al fin thickness using the Levelized Cost of Energy (LCOE) calculations, were evaluated. The cost analysis included the three different al fin thickness ECT. And the initial investment and setup costs includes:

1. Cost of the Al fin solar absorber
2. Cost of the solar paint
3. Cost of the ETC

The initial costs of the project (Year 0) were 569.35 dollar (11 μm), 571.55 dollar (13 μm) and 583.61dollar (24 μm) as shown in the table 10-11. Operating and maintenance cost 0.5% and salvage cost 10% of the initial investment cost salvage cost was considered. The operating and maintenance costs for the 16 years of expected operating life were 26 dollars each for 11 and 13 μm and 27 dollars for 24 μm . These costs included the projected annual electricity cost, maintenance cost, replacement parts cost and miscellaneous operating costs.

For years 1-15 the projected costs were discounted back to present value by a NPV calculation formula with a discount rate of 7%.

Estimates of Benefits from the system included the salvage value 10% of initial cost were 20.64 dollar (11 μm), 20.72 dollar (13 μm) and 21.15 dollar (24 μm). The annual heat production of the various systems was estimated 3181.34 MJ (11 μm), 2949MJ (13 μm) and 2327.27MJ (24 μm). Electric hot water systems of comparative annual heat production consumed 818.25 kWh, 758.61 kWh and 598.58 kWh respectively. If these energies converted in terms of money by multiplying the energy by the current electric tariff in Thailand $4.22 \text{ Baht}/35.4 = 0.12 \text{ dollar per kWh}$ will be 98.19, 91.03 and 71.83 dollars respectively will be saved annually.

Table 10 Investment cost and benefit of the project

Details		Value (Dollar)
Investment costs		
cost of the evacuated tube collector		440
Aluminum fin	11 (1set/ 15 pieces)	11.85
	13 (1set/ 15 pieces)	14.05
	24 (1set/15 pieces)	26.11
shipment		70
painting per sample		1288.75 THB/35.4 = 36
thinner per sample		406.97 THB/35.4= 11.50
total investment		569.35; 571.55; 583.61
Operating and Maintenance Cost 0.5%		
11		26
13		26
24		27
Benefit		
Energy Produce		MJ
11		3181.34
13		2949.50
24		2327.27
Salvage value		Dollar
11		20.64
13		20.72
24		21.15

Table 11 The parameters for calculation

Parameter	Symbol	Thickness (μm)			Unit
		11	13	24	
Investment and setup costs	C_e	569.35	571.55	583.65	Dollar
Operating and maintenance cost	C_n	2.85	2.86	2.92	Dollar
Salvage value	SV	56.94	57.16	58.36	Dollar
The annual heat production	E_n	883.71.20	819.30	646.46	KWh/Year
Discount rate	i	7	7	7	%
Life time	n	16	16	16	Year
Number of Years	N	15	15	15	Year

Table 12 Values of parameters for calculating the energy yield

Parameter	Symbol	Value	Unit
Global radiation	G_t	800	W/m^2
Ambient temperature	T_a	30	C
Water inlet temperature	T_i	35	C
Water outlet temperature	T_o	60	C
Average Global solar radiation in Thailand	E	1800	$\text{kWh/m}^2.\text{year}$

Using the values mentioned in table 12 to calculate the annual energy output of the experimental ETC with an Al fin thickness of 11 μm as the solar absorber will be:

The thermal efficiency equation

$$\eta = 0.55 - 15.74 \left[\frac{(T_i - T_a)}{G_t} \right] - 14.23 \left[\frac{(T_i - T_a)^2}{G_t^2} \right]$$

Calculation with parameters from the above table

$$\eta = 0.55 - 15.74 * \left[\frac{(35 - 30)}{800} \right] - 14.23 * \left[\frac{(35 - 30)^2}{800^2} \right]$$

$$\eta = 0.45$$

$$\text{Annual energy calculations} = 0.45 * E \text{ kWh/m}^2.\text{Year}$$

$$= 0.45 \times 1800 \text{ kWh/m}^2 \cdot \text{Year}$$

$$= 818.25 \text{ kWh/m}^2 \cdot \text{Year}$$

The Table 13 summarizes the annual energy output for each thickness of the Al fin used.

Table 13 Annual yield energy from ETC

Al fin thickness (μm)	Annual Energy Yield (kWh/m^2)	Annual Energy Yield (kWh)	Annual Energy Yield (MJ)
11	818.25	883.71	3181.34
13	758.62	819.30	2949.50
24	598.58	646.46	2327.27

Table 14 The LCOE of the ETC using Al fin of 11 μm thickness as solar absorber

Year	Initial cost	O&M (0.5%)	Salvage value (10%)	O&M cost (NPV)	Salvage value (NPV)	Energy Production
0	569.35					
1		2.85		3		818.247
2		2.85		2		818.247
3		2.85		2		818.247
4		2.85		2		818.247
5		2.85		2		818.247
6		2.85		2		818.247
7		2.85		2		818.247
8		2.85		2		818.247
9		2.85		2		818.247
10		2.85		1		818.247
11		2.85		1		818.247
12		2.85		1		818.247
13		2.85		1		818.247
14		2.85		1		818.247
15		2.85	56.935	1	20.63586	818.247
Total	569			26		12273.7
LCOE					0.05 dollar/kWh	

Table 15 The LCOE of the ETC using Al fin of 13 μm thickness as solar absorber

Year	Initial cost	O&M (0.5%)	Salvage value10%	O&M cost (NPV)	Salvage value (NPV)	Energy Production
0	571.55					
1		2.86		3		758.6153
2		2.86		2		758.6153
3		2.86		2		758.6153
4		2.86		2		758.6153
5		2.86		2		758.6153
6		2.86		2		758.6153
7		2.86		2		758.6153
8		2.86		2		758.6153
9		2.86		2		758.6153
10		2.86		1		758.6153
11		2.86		1		758.6153
12		2.86		1		758.6153
13		2.36		1		758.6153
14		2.86		1		758.6153
15		2.86	57.155	1	20.7156	758.6153
Total	572			26		11379.23
LCOE					0.05 dollars /kWh	

Table 16 The LCOE of the ETC using Al fin of 24 μm thickness as solar absorber

Year	Initial cost	O&M (0.5%)	Salvage value 10%	O&M cost (NPV)	Salvage value (NPV)	Energy Production
0	583.61					
1		2.92		3		598.576289
2		2.92		2		598.576289
3		2.92		2		598.576289
4		2.92		2		598.576289
5		2.92		2		598.576289
6		2.92		2		598.576289
7		2.92		2		598.576289
8		2.92		1		598.576289
9		2.92		1		598.576289
10		2.92		1		598.576289
11		2.92		1		598.576289
12		2.92		1		598.576289
13		2.92		1		598.576289
14		2.92		1		598.576289
15		2.92	58.36	1	21.15	598.576289
Total	583.61			27		8978.64434
LCOE					0.07 dollars /kWh	

The LCOE for the three different Al fin absorber thickness considered are computed after the calculation of present value of salvage and operation and maintenance value of all samples which their values are mentioned in Table 14-16. And the values of LCOE are 0.05 dollars/kWh for 11 and 13 μm and 0.07 dollars /kWh for 24 μm . As the energy production and initial cost for 11 and 13 m Al fin is close to each other, their LCOE comes to be equal. When it compares with 24 μm it increased by 75%.

CHAPTER V

CONCLUSION

The conclusions and recommendations of this research are described in this chapter.

Conclusions

Coating Thickness

The thickness of the solar paint measured using Physic min 730 digital device, shows a significant difference in their thickness among single, double and triple layer. But generally the paint thicknesses value is low. After the application of paint to the Al absorber and given a considerable time for drying, the paint was observed to scratch easily especially during the inserting to the evacuated double glass tube, and this shows the paint has weak bondage to the surface of Al absorber.

Optical Characterization of the coated Al fin

UV Vis NIR test

The results from the solar reflectance measurements over 250-2500 nm. wavelengths for the three different paint thickness samples shows almost the same value of reflectance and calculated value of absorptance ($\alpha = 0.94$), even though the thicker one 0.2% more value in absorptance (where the solar intensity is low) compared with the others, it is not justifiable to coat with the absorber fin with triple layer. So single layer is chosen to apply on the real al fin absorber.

XRD analysis

From the XRD result, only the Al element appear on the surface which shows the function of the coating was suppressed due to low bondage and low quantity of the solar paint. And this may have an adverse effect on transferring the heat energy from the coating toward the Al absorber and this easily can be confirmed from the low value of the heat removal factor and low thermal efficiency compared to the previous researcher.

Outdoor ETC performance test

The performance of the ETC varies as the thickness of the Al fin absorber thicknesses varies, and generally the relation is as the thickness increases the thermal efficiency of the ETC decreases and this goes matches with one dimensional heat conduction formula (Planck's formula) which shows the relation between thickness of material and heat transfer rate is inversely in one dimensional heat transfer case. The thinner Al fin (11 μm) is preferred to use in the ETC application.

Levelized cost of energy, LCOE analysis

It shows a little difference of LCOE between 11,13 μm with 24 μm Al fin. Even though the benefit is not much it is economically advantageous when the ETC uses thinner Al fin.

Recommendations

From this experiment solar paint may also be recommended for using in solar air dryer application as the energy need not to transfer to the substrate absorber material.

Even though the 11micron Al fin is almost the thinnest fin, to go for lower than this thickness, further study is required as solar absorber should be durable in strength wise, which might be difficult to find a durable Al fin with thickness less than this.



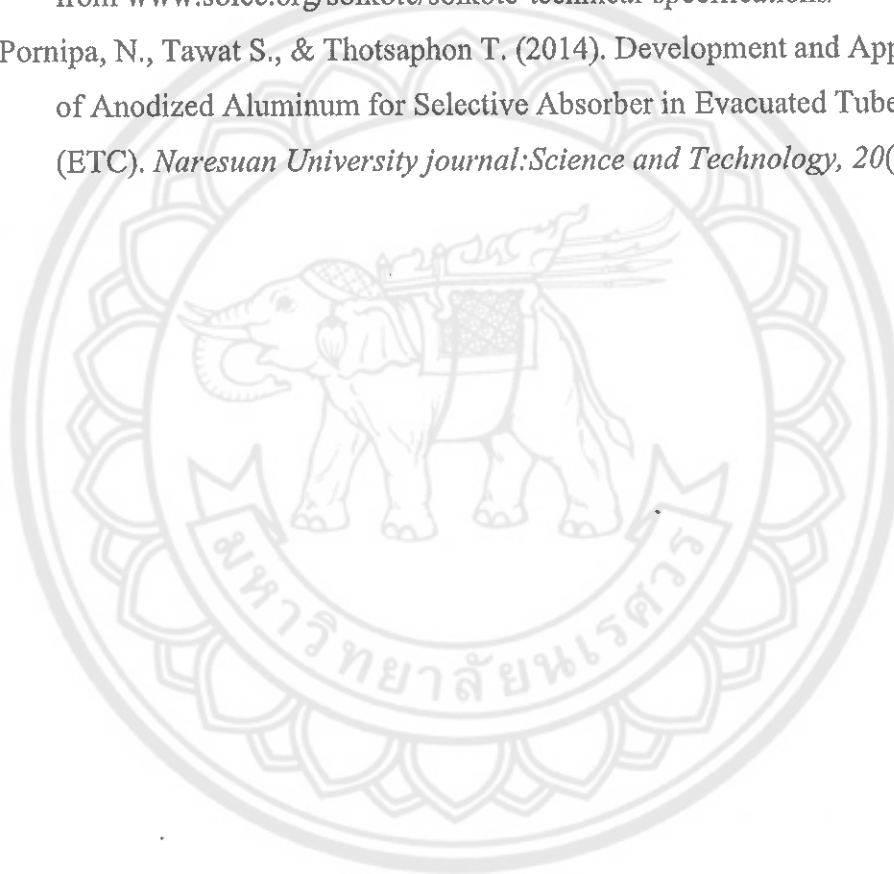
REFERENCES

- [1] Faizal, M., Saidur, R., Mekhilef, S., & Alim, M.A. (2013). Energy, economic and environmental analysis of metal oxides nanofluid for flat-plate solar collector. *Energy Conversion and Management*, 76, 162-168.
- [2] Del Col, D., Padovan, A., Bortolato, M., Dai Prè, M., & Zambolin, E. (2013). Thermal performance of flat plate solar collectors with sheet-and-tube and roll-bond absorbers. *Energy*, 58, 258-269.
- [3] Jyothi, J., Chaliyawala, H., Srinivas, G., Nagaraja, H.S., & Barshilia, H.C. (2015). Design and fabrication of spectrally selective TiAlC/TiAlCN/TiAlSiCN/TiAlSiCO/TiAlSiO tandem absorber for high-temperature solar thermal power applications. *Solar Energy Materials and Solar Cells*, 140, 209-216.
- [4] Farooq, M., & Hutchins, M.G. (2002). A novel design in composites of various materials for solar selective coatings. *Solar Energy Materials and Solar Cells*, 71(4), 523-535.
- [5] Suman, S., Khan, M.K., & Pathak, M. (2015). Performance enhancement of solar collectors—A review. *Renewable and Sustainable Energy Reviews*, 49, 192-210.
- [6] Tesfamichael, T. (2000). *Characterization of Selective Solar Absorbers: Experimental and theoretical modeling* (Doctoral dissertation). Sweden: University of Uppsala.
- [7] Kalogirou, S.A. (2004). Solar thermal collectors and applications. *Progress in Energy and Combustion Science*, 30(3), 231-295.
- [8] Sabiha, M.A., Saidur, R., Mekhilef, S., & Mahian, O. (2015). Progress and latest developments of evacuated tube solar collectors. *Renewable and Sustainable Energy Reviews*, 51, 1038-1054.
- [9] Apricus Solar Hot Water. (2010). *ETC-DEMO with labels*. Retrieved September 5, 2016, from http://www.apricus.com/html/solar_collector.htm#VwirMKR96hc
- [10] Morrison, G.L., Budihardjo, I., & Behnia, M. (2004). Water-in-glass evacuated tube solar water heaters. *Solar Energy*, 76(1-3), 135-140.

- [11] Ma, L., Lu, Z., Zhang, J., & Liang, R. (2010). Thermal performance analysis of the glass evacuated tube solar collector with U-tube. *Building and Environment*, 45(9), 1959-1967.
- [12] Sharma, N., & Diaz, G. (2011). Performance model of a novel evacuated-tube solar collector based on minichannels. *Solar Energy*, 85(5), 881-890.
- [13] ISO. (1992). *ISO 9845-1:1992*. Retrieved April 5, 2016, from <https://www.iso.org/standard/17723.html>
- [14] Wijewardane, S., & Goswami, D.Y. (2012). A review on surface control of thermal radiation by paints and coatings for new energy applications. *Renewable and Sustainable Energy Reviews*, 16(4), 1863-1873.
- [15] Akhtarkhavari, A., Kortschot, M.T., & Spelt, J.K. (2004). Adhesion and durability of latex paint on wood fiber reinforced polyethylene. *Progress in Organic Coatings*, 49(1), 33-41.
- [16] Hazami, M., Kooli, S., Naili, N., & Farhat, A. (2013). Long-term performances prediction of an evacuated tube solar water heating system used for single-family households under typical Nord-African climate (Tunisia). *Solar Energy*, 94, 283-298.
- [17] Gao, Y., Zhang, Q., Fan, R., Lin, X., & Yu, Y. (2013). Effects of thermal mass and flow rate on forced-circulation solar hot-water system: Comparison of water-in-glass and U-pipe evacuated-tube solar collectors. *Solar Energy*, 98, 290-301.
- [18] Ayompe, L. M., & Duffy, A. (2013). Thermal performance analysis of a solar water heating system with heat pipe evacuated tube collector using data from a field trial. *Solar Energy*, 90, 17-28.
- [19] Yamaguchi, H., Sawada, N., Suzuki, H., Ueda, H., & Zhang, X.R. (2010). Preliminary Study on a Solar Water Heater Using Supercritical Carbon Dioxide as Working Fluid. *Journal of Solar Energy Engineering*, 132(1), 011010.
- [20] Morrison, G. L., Budihardjo, I., & Behnia, M. (2005). Measurement and simulation of flow rate in a water-in-glass evacuated tube solar water heater. *Solar Energy*, 78(2), 257-267.

- [21] Orel, Z., Gunde, M., Lenček, A., & Benz, N. (2001). The preparation and testing of spectrally selective paints on different substrates for solar absorbers. *Solar Energy*, 69, Supplement 6, 131-135.
- [22] Gunde, M. K., Orel, Z.C., & Hutchins, M.G. (2003). The influence of paint dispersion parameters on the spectral selectivity of black-pigmented coatings. *Solar Energy Materials and Solar Cells*, 80(2), 239-245.
- [23] Kunič, R., Mihelčič, M., Orel, B., Slemenik Perše, L., Bizjak, B., Kovač, J., & Brunold, S. (2011). Life expectancy prediction and application properties of novel polyurethane based thickness sensitive and thickness insensitive spectrally selective paint coatings for solar absorbers. *Solar Energy Materials and Solar Cells*, 95(11), 2965-2975.
- [24] Orel, B., Spreizer, H., Slemenik Perše, L., Fir, M., Šurca Vuk, A., Merlini, D., . . . Köhl, M. (2007). Silicone-based thickness insensitive spectrally selective (TISS) paints as selective paint coatings for coloured solar absorbers (Part I). *Solar Energy Materials and Solar Cells*, 91(2-3), 93-107.
- [25] Lundh, M., Blom, T., & Wäckelgård, E. (2010). Antireflection treatment of Thickness Sensitive Spectrally Selective (TSSS) paints for thermal solar absorbers. *Solar Energy*, 84(1), 124-129.
- [26] Orel, B., Spreizer, H., Šurca Vuk, A., Fir, M., Merlini, D., Vodlan, M., & Köhl, M. (2007). Selective paint coatings for coloured solar absorbers: Polyurethane thickness insensitive spectrally selective (TISS) paints (Part II). *Solar Energy Materials and Solar Cells*, 91(2-3), 108-119.
- [27] Orel, Z., & Gunde, M. (2000). Spectrally selective paint coatings preparation and characterization. *Solar Energy Materials & Solar Cells*, 68, 337-353.
- [28] ASM. (2017). *Aluminum 6061-T6*. Retrieved September 5, 2016, from <http://asm.matweb.com/search/SpecificMaterial.asp?bassnum=ma6061t6>
- [29] Dampaney Company Inc. (2016). *Thurmalox 250-Solar Coating*. Retrieved May 5, 2016, from <http://www.dampney.com/Product-Line/AT/View/PID/2/Thurmalox-250>
- [30] Combrdige Glassblowing. (2015). *Glass Properties*. Retrieved January 15, 2017, from <http://www.camglassblowing.co.uk/glass-properties/>

- [31] ISO. (1994). *ISO 9806-1:1994*. Retrieved June 10, 2016, from <https://infostore.saiglobal.com/store/details.aspx?ProductID=377243>
- [32] Liu, Y., Wang, Z., Lei, D., & Wang, C. (2014). A new solar spectral selective absorbing coating of SS-(Fe₃O₄)/Mo/TiZrN/TiZrON/SiON for high temperature application. *Solar Energy Materials and Solar Cells*, 127, 143-146.
- [33] SOLEC. (2016). *Solkote Selective Solar Coating*. Retrieved November 4, 2016, from www.solec.org/solkote/solkote-technical-specifications/
- [34] Pornipa, N., Tawat S., & Thotsaphon T. (2014). Development and Application of Anodized Aluminum for Selective Absorber in Evacuated Tube Collector (ETC). *Naresuan University journal: Science and Technology*, 20(1), 16-23.





APPENDIX A

Table 17 Paint thickness at different position for sample of single layer coating

Roll No.	Thickness (μm)	Roll No.	Thickness (μm)	Roll No.	Thickness (μm)
1	0.25	18	5.9	35	7.95
2	0.4	19	4.9	36	5.2
3	0.5	20	4.2	37	9.85
4	2.05	21	1.8	38	3.3
5	3.35	22	2.0	39	1.6
6	4.85	23	4.8	40	2.95
7	5.3	24	4.65	41	8.1
8	6.0	25	7.25	42	7.05
9	4.7	26	1.1	43	19.3
10	1.75	27	3.6	44	8.8
11	2.6	28	3.5	45	9.95
12	1.25	29	5.65	46	8.05
13	2.45	30	6.4	47	8.15
14	1.8	31	2.8	48	4.65
15	5.45	32	2.3	49	2.25
16	6.55	33	3.5	50	2.85
17	6.8	34	7.6		

Average thickness is 4.76 μm

Table 18 Paint thickness at different position for sample of double layer coating

Roll No.	Thickness (μm)	Roll No.	Thickness (μm)	Roll No.	Thickness (μm)
1	6.2	18	2.55	35	3.95
2	5.6	19	3.05	36	6
3	4.9	20	4.2	37	6.95
4	3.1	21	7	38	6.75
5	6.15	22	8.25	39	4.7
6	6.4	23	6.75	40	5.4
7	5.7	24	7.05	41	5.35
8	8.65	25	6.6	42	5.2
9	8.55	26	5.25	43	5.5
10	7.9	27	6.4	44	4.65
11	9.5	28	7.9	45	11.1
12	6.1	29	5.6	46	5.3
13	4.85	30	6.05	47	7.2
14	4.7	31	2.55	48	3.95
15	4.45	32	3.3	49	4.35
16	7.4	33	7	50	5.65
17	7.8	34	4.55		

Average thickness is 5.88 μm

Table 19 Paint thickness at different position for sample of triple layer coating

Roll No.	Thickness (μm)	Roll No.	Thickness (μm)	Roll No.	Thickness (μm)
1	10.55	18	13.9	35	9.05
2	10.25	19	14.6	36	8.55
3	17.8	20	14.6	37	8.7
4	12.6	21	11.3	38	8.95
5	13.3	22	11.2	39	8.9
6	10.45	23	14.1	40	8.05
7	10.85	24	14.85	41	11.35
8	10.3	25	11.45	42	11.25
9	10.15	26	10.05	43	10.4
10	10.5	27	10.4	44	10.95
11	12.2	28	11.4	45	13.55
12	10.75	29	10.35	46	13.15
13	11.65	30	7.4	47	9.35
14	10.8	31	7.75	48	10.5
15	11.8	32	8.35	49	10.75
16	13.75	33	10.75	50	11.95
17	13.6	34	9.55		

Average thickness is 11.174 μm

APPENDIX B

Powder –Diffract-File from JCPDS-ICDD

Name and formula

Reference code:	00-001-1176
PDF index name:	Aluminum
Empirical formula:	Al
Chemical formula:	Al

Crystallographic parameters

Crystal system:	Cubic
Space group:	Fm3m
Space group number:	225
a (?):	4.0406
b (?):	4.0406
c (?):	4.0406
Alpha (?):	90.0000
Beta (?):	90.0000
Gamma (?):	90.0000
Measured density (g/cm ³):	2.69
Volume of cell (10 ⁶ pm ³):	65.97
Z:	4.00
RIR:	-

Status, subfiles and quality

Status:	Marked as deleted by ICDD
Subfiles:	Inorganic
Quality:	Blank (B)

Comments

Deleted by:	Deleted by NBS card.
Color:	White
Melting point:	660

References

Primary reference:

Davey., *Phys. Rev.*, **25**, 753, (1925)

Optical data:

Data on Chem. for Cer. Use, Natl. Res. Council Bull. 107

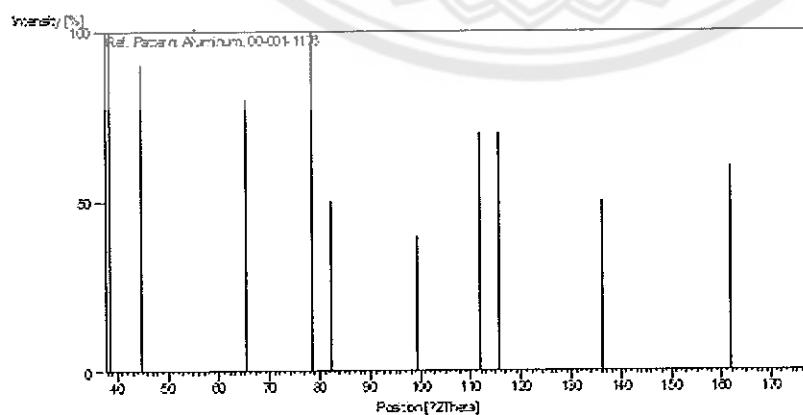
Unit cell:

The Structure of Crystals, 1st Ed.

Peak list

No.	h	k	l	d [Å]	2Theta[deg]	I [%]
1	1	1	1	2.34	38.439	100
2	2	0	0	2.02	44.833	90
3	2	2	0	1.43	65.186	80
4	3	1	1	1.22	78.306	100
5	2	2	2	1.17	82.352	50
6	4	0	0	1.01	99.401	40
7	3	3	1	0.93	111.845	70
8	4	2	0	0.91	115.662	70
9	4	2	2	0.83	136.273	50
10	5	1	1	0.78	161.909	60
11				0.72		20

Stick Pattern



Name and formula

Reference code:	00-001-1243
PDF index name:	Aluminum Oxide
Empirical formula:	Al ₂ O ₃
Chemical formula:	Al ₂ O ₃

Crystallographic parameters

Crystal system:	Rhombohedral
Space group:	R-3c
Space group number:	167
a (?):	4.7500
b (?):	4.7500
c (?):	12.9700
Alpha (?):	90.0000
Beta (?):	90.0000
Gamma (?):	120.0000
Measured density (g/cm ³):	4.02
Volume of cell (10 ⁶ pm ³):	253.43
Z:	2.00
RIR:	

Status, subfiles and quality

Status:	Marked as deleted by ICDD
Subfiles:	Inorganic Alloy, metal or intermetallic
Quality:	Blank (B)

Comments

Deleted by:	Deleted by NBS.
Color:	Various
Optical data:	A=1.7604, B=1.7686, Sign=-
Melting point:	2050
Unit cell:	Rhombohedral cell: a=5.120, a=55.28.

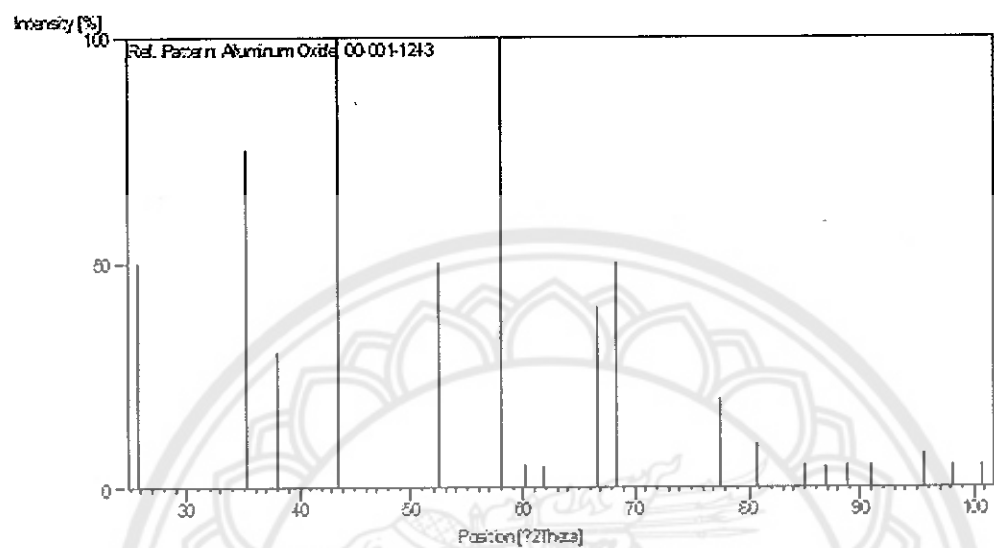
References

Primary reference: Hanawalt et al., *Anal. Chem.*, **10**, 475, (1938)

Unit cell: *Dana's System of Mineralogy, 7th Ed.*

Peak list

<u>No.</u>	<u>h</u>	<u>K</u>	<u>I</u>	<u>d [Å]</u>	<u>2Theta[deg]</u>	<u>I [%]</u>
1	0	1	2	3.4700	25.652	50.0
2	1	0	4	2.5500	35.165	75.0
3	1	1	0	2.3700	37.934	30.0
4	1	1	3	2.0800	43.473	100.0
5	0	2	4	1.7400	52.553	50.0
6	1	1	6	1.5900	57.955	100.0
7	2	1	1	1.5400	60.026	5.0
8	0	1	8	1.5000	61.799	5.0
9	2	1	4	1.4000	66.763	40.0
10	3	0	0	1.3700	68.425	50.0
11	1	1	9	1.2300	77.549	20.0
12	2	1	7	1.1900	80.678	10.0
13	1	3	1	1.1400	85.017	5.0
14	1	2	8	1.1200	86.907	5.0
15	0	2	10	1.1000	88.898	5.0
16	0	0	12	1.0800	90.998	5.0
17	2	2	6	1.0400	95.578	8.0
18	0	4	2	1.0200	98.085	5.0
19	2	1	10	1.0000	100.762	5.0

Stick Pattern

APPENDIX C

Table 20 The calculation of the solar absorptance of solar paint coated Al fin single layer

Wavelength nm	Direct circumsolar $W \cdot m^{-2} \cdot nm^{-1}$	I_{sol}	I_{sol} $W \cdot m^{-2}$	Reflectanc e (1)	$1-R(\lambda)$	Integrate $I_{sol} \cdot (1-R) d\lambda$ $\int_{300}^{2500} I_{sol} (1-R(\lambda)) d\lambda$	Integrate I_{sol} $\int_{300}^{2500} I_{sol}(\lambda) d\lambda$	Absorptanc	
								e %	Absorptance* I_{sol} (%)
λ	I_{sol}	$I_{sol}(\lambda)$	R					α	
300	4.56E-04	1.37E-01	0.0642	0.93585					
301	9.19E-04	2.77E-01	0.0642	0.93582	0.0006	0.0007		93.5830	8.60E-04
302	1.46E-03	4.40E-01	0.0642	0.93576	0.0011	0.0012		93.5783	1.36E-03
303	3.73E-03	1.13E+00	0.0641	0.93587	0.0024	0.0026		93.5839	3.49E-03
304	5.10E-03	1.55E+00	0.0641	0.93587	0.0041	0.0044		93.5870	4.77E-03
305	8.93E-03	2.72E+00	0.0642	0.93585	0.0066	0.0070		93.5857	8.36E-03
306	1.02E-02	3.11E+00	0.0640	0.93599	0.0089	0.0095		93.5924	9.50E-03
307	1.52E-02	4.68E+00	0.0641	0.93594	0.0119	0.0127		93.5960	1.43E-02
308	2.08E-02	6.39E+00	0.0641	0.93593	0.0168	0.0180		93.5934	1.94E-02
309	2.23E-02	6.89E+00	0.0639	0.9361	0.0201	0.0215		93.6018	2.09E-02
310	2.78E-02	8.63E+00	0.0638	0.9362	0.0235	0.0251		93.6156	2.60E-02

Table 20 (cont.)

Wavelength	Direct circumsolar	I_{sol}	Reflectan	$1-R(\lambda)$	integrate	integrate	Absorptanc	Absorptanc* I_{sol}
nm	$W \cdot m^{-2} \cdot nm^{-1}$	$W \cdot m^{-2}$	ce (1)		$I_{sol}^* (1-R)$	$R \cdot d\lambda$	%	(%)
λ	I_{sol}	$I_{sol}(\lambda)$	R		$\int_{300}^{2500} I_{sol} (1-R(\lambda)) d\lambda$	$\int_{300}^{2500} I_{sol}(\lambda) d\lambda$	α	
311	4.54E-02	1.41E+01	0.0638	0.93623	0.0343	0.0366	93.6219	4.25E-02
312	5.09E-02	1.59E+01	0.0636	0.93637	0.0451	0.0481	93.6304	4.77E-02
.
.
2475	1.64E-02	4.05E+01	0.4418	0.55821	0.0463	0.0825	56.0796	9.18E-03
2480	8.00E-03	1.98E+01	0.4470	0.55305	0.0339	0.0609	55.6516	4.45E-03
2485	5.58E-03	1.39E+01	0.4519	0.54814	0.0187	0.0340	55.1032	3.08E-03
2490	3.50E-03	8.70E+00	0.4565	0.54355	0.0124	0.0227	54.6373	1.91E-03
2495	2.86E-03	7.15E+00	0.4607	0.53931	0.0086	0.0159	54.1640	1.55E-03
2500	7.03E-03	1.76E+01	0.4644	0.53558	0.0133	0.0247	53.6660	3.77E-03
Total					838.4384	892.2869	0.9397	

Table 21 The calculation of the solar absorptance of solar paint coated Al fin double layer

Wavelength nm	Direct circumsolar $W \cdot m^{-2} \cdot nm^{-1}$	Reflectan			Absorptanc		
		I_{sol}	ce (1)	$1-R(\lambda)$	integrate I_{sol}	integrate $I_{sol} \cdot (1-R)$	Absorptance* I_{sol} %
λ	I_{sol}	$W \cdot m^{-2}$	R	$1-R(\lambda)$	$\int_{300}^{2500} I_{sol} (1-R(\lambda)) d\lambda$	$\int_{300}^{2500} I_{sol} (1-R(\lambda)) d\lambda$	α
300	4.56E-04	1.37E-01	0.0651	0.935	0.0007	0.0007	93.4950
301	9.19E-04	2.77E-01	0.0651	0.935	0.0006	0.0006	8.59E-04
302	1.46E-03	4.40E-01	0.0651	0.935	0.0011	0.0012	1.36E-03
303	3.73E-03	1.13E+00	0.0652	0.935	0.0024	0.0026	3.49E-03
304	5.10E-03	1.55E+00	0.0650	0.935	0.0041	0.0044	4.77E-03
305	8.93E-03	2.72E+00	0.0649	0.935	0.0066	0.0070	8.35E-03
306	1.02E-02	3.11E+00	0.0650	0.935	0.0089	0.0095	9.49E-03
307	1.52E-02	4.68E+00	0.0649	0.935	0.0119	0.0127	1.43E-02
308	2.08E-02	6.39E+00	0.0648	0.935	0.0168	0.0180	1.94E-02
309	2.23E-02	6.89E+00	0.0647	0.935	0.0201	0.0215	2.09E-02
310	2.78E-02	8.63E+00	0.0646	0.935	0.0234	0.0251	2.60E-02

Table 21 (cont.)

Wavelength nm	Direct circumsolar $W \cdot m^{-2} \cdot nm^{-1}$	I_{sol} $W \cdot m^{-2}$	Reflectan		Absorptanc e	Absorptanc* I_s ol
			ce (1)	$1-R(\lambda)$ $\int_{300}^{2500} I_{sol} (1-R(\lambda)) d\lambda$ R	integrate I_{sol} $\int_{300}^{2500} I_{sol}(\lambda) d\lambda$	ol (%)
λ	I_{sol}	$I_{sol}(\lambda)$			α	
311	4.54E-02	1.41E+01	0.0646	0.935	0.0366	93.5384 4.25E-02
312	5.09E-02	1.59E+01	0.0644	0.936	0.0481	93.5517 4.76E-02
.
.
2475	1.64E-02	4.05E+01	0.4823	0.518	0.0825	52.0563 8.52E-03
2480	8.00E-03	1.98E+01	0.4876	0.512	0.0609	51.5967 4.13E-03
2485	5.58E-03	1.39E+01	0.4931	0.507	0.0340	51.0128 2.85E-03
2490	3.50E-03	8.70E+00	0.4986	0.501	0.0227	50.4786 1.76E-03
2495	2.86E-03	7.15E+00	0.5030	0.497	0.0159	49.9401 1.43E-03
2500	7.03E-03	1.76E+01	0.5080	0.492	0.0247	49.3422 3.47E-03
		Total		835.7525	892.2869	0.9366

Table 22 The calculation of the solar absorptance of solar paint coated Al fin triple layer

Wavelength nm	Direct circumsolar $W^*m^{-2}nm^{-1}$	I_{sol} W^*m^{-2}	Reflectance (1)	$1-R(\lambda)$	integrate $I_{sol}*(1-R)d\lambda$ \int_{300}^{2500}	integrate I_{sol} $\int_{300}^{2500} I_{sol}(\lambda)d\lambda$	Absorbance %	Absorbance* I_{sol} (%)
λ	I_{sol}	$I_{sol}(\lambda)$	R			α		
300	4.56E-04	1.37E-01	0.0665	0.934			93.3520	8.58E-04
301	9.19E-04	2.77E-01	0.0665	0.934	0.0006	0.0007	93.3426	1.36E-03
302	1.46E-03	4.40E-01	0.0666	0.933	0.0011	0.0012	93.3396	3.48E-03
303	3.73E-03	1.13E+00	0.0666	0.933	0.0024	0.0026	93.3404	4.76E-03
304	5.10E-03	1.55E+00	0.0666	0.933	0.0041	0.0044	93.3425	8.34E-03
305	8.93E-03	2.72E+00	0.0666	0.933	0.0065	0.0070	93.3408	9.47E-03
306	1.02E-02	3.11E+00	0.0666	0.933	0.0089	0.0095	93.3452	1.42E-02
307	1.52E-02	4.68E+00	0.0665	0.934	0.0119	0.0127	93.3552	1.94E-02
308	2.08E-02	6.39E+00	0.0664	0.934	0.0168	0.0180	93.3621	2.08E-02
309	2.23E-02	6.89E+00	0.0664	0.934	0.0201	0.0215	93.3678	2.60E-02
310	2.78E-02	8.63E+00	0.0663	0.934	0.0234	0.0251		

Table 22 (cont.)

Wavelength nm	Direct circumsolar $W^*m^{-2}nm^{-1}$	I_{sol} W^*m^{-2}	Reflectance (1)	$1-R(\lambda)$	integrate $I_{sol}*(1-R)d\lambda$ $\int_{300}^{2500} I_{sol} (1-R(\lambda))d\lambda$	integrate I_{sol} $\int_{300}^{2500} I_{sol}(\lambda)d\lambda$	Absorbance %	Absorbance* I_{sol} (%)
λ	I_{sol}	$I_{sol}(\lambda)$	R			α		
311	4.54E-02	1.41E+01	0.0663	0.934	0.0342	0.0366	93.3700	4.24E-02
312	5.09E-02	1.59E+01	0.0661	0.934	0.0450	0.0481	93.3827	4.75E-02
.
.
2475	1.64E-02	4.05E+01	0.2515	0.749	0.0619	0.0825	75.0269	1.23E-02
2480	8.00E-03	1.98E+01	0.2552	0.745	0.0455	0.0609	74.7306	5.98E-03
2485	5.58E-03	1.39E+01	0.2599	0.740	0.0252	0.0340	74.2848	4.15E-03
2490	3.50E-03	8.70E+00	0.2639	0.736	0.0168	0.0227	73.8559	2.58E-03
2495	2.86E-03	7.15E+00	0.2670	0.733	0.0117	0.0159	73.4729	2.10E-03
2500	7.03E-03	1.76E+01	0.2690	0.731	0.0181	0.0247	73.1556	5.14E-03
		Total			840.0229	892.2869	0.9414	

APPENDIX D

Table 23 The thermal efficiency of ETC with 24 μm Al fin absorber

T_{in} (°C)	T_{out} (°C)	T_{am} (°C)	G_t (W/m ²)	$(T_{in}-T_{am})/G_t$	η
30.47	32.51	25.73	907.73	0.00522	0.344
30.53	32.44	25.76	907.93	0.00525	0.323
30.50	32.45	25.83	909.42	0.00513	0.329
30.50	32.48	25.90	910.25	0.00505	0.334
30.47	32.48	25.99	909.64	0.00492	0.340
30.54	32.51	25.99	910.75	0.00499	0.333
30.56	32.49	26.12	909.80	0.00488	0.324
30.50	32.48	26.15	911.47	0.00477	0.333
30.60	32.52	26.02	911.13	0.00502	0.324
30.46	32.54	25.93	911.37	0.00497	0.350
30.55	32.54	25.98	911.72	0.00501	0.334
30.59	32.49	26.05	911.74	0.00497	0.319
30.59	32.56	25.98	911.35	0.00506	0.331
30.62	32.52	25.95	913.17	0.00511	0.319
30.60	32.60	26.06	911.48	0.00497	0.336
30.73	32.71	26.11	913.96	0.00505	0.333
30.75	32.71	26.24	914.68	0.00492	0.328
30.80	32.75	26.12	914.72	0.00512	0.326
40.05	41.53	26.69	940.57	0.01421	0.240
40.08	41.73	26.72	941.70	0.01419	0.268
40.03	41.52	26.98	931.04	0.01402	0.244
40.17	41.70	27.38	928.85	0.01378	0.252
40.04	41.64	27.39	925.28	0.01367	0.265
40.09	41.66	27.45	921.53	0.01372	0.260
40.10	41.65	27.42	917.88	0.01381	0.258

Table 23 (cont.)

$T_{in} (^{\circ}\text{C})$	$T_{out} (^{\circ}\text{C})$	$T_{am} (^{\circ}\text{C})$	$G_t (\text{W/m}^2)$	$(T_{in}-T_{am})/G_t$	η
40.07	41.70	27.30	915.53	0.01395	0.273
40.21	41.85	27.28	906.79	0.01426	0.277
40.19	41.75	27.28	905.49	0.01426	0.264
40.27	41.74	27.28	913.96	0.01422	0.246
40.42	42.00	27.29	928.28	0.01414	0.260
40.37	41.99	27.35	923.06	0.01410	0.269
40.39	41.97	27.57	928.72	0.01380	0.262
40.47	42.01	27.42	923.53	0.01413	0.255
40.60	42.15	27.39	920.95	0.01435	0.257
40.54	42.02	27.42	917.29	0.01431	0.247
40.53	42.07	27.32	925.92	0.01427	0.255
50.86	51.77	27.98	926.66	0.02470	0.150
50.43	51.25	27.82	933.60	0.02422	0.135
50.44	51.39	27.81	934.52	0.02422	0.155
50.53	51.39	27.88	936.13	0.02420	0.139
50.58	51.43	27.95	935.94	0.02419	0.138
50.51	51.40	27.95	929.63	0.02427	0.147
50.70	51.49	28.04	931.54	0.02433	0.130
50.83	51.81	28.07	930.78	0.02445	0.162
50.75	51.59	28.06	931.81	0.02435	0.139
50.73	51.68	28.06	932.30	0.02431	0.157
50.66	51.70	28.01	931.36	0.02432	0.172
50.57	51.57	28.04	930.63	0.02421	0.165
50.66	51.65	28.05	931.31	0.02427	0.164
50.72	51.57	28.04	933.64	0.02428	0.140
50.73	51.53	28.10	933.36	0.02424	0.132
50.79	51.60	28.09	931.29	0.02437	0.134
50.97	51.81	28.17	925.75	0.02463	0.139

Table 23 (cont.)

T_{in} (°C)	T_{out} (°C)	T_{am} (°C)	G_t (W/m ²)	$(T_{in}-T_{am})/G_t$	η
50.89	51.84	28.25	922.16	0.02455	0.159
60.50	60.98	30.41	930.50	0.03234	0.078
60.46	61.00	30.37	929.22	0.03238	0.089
60.48	60.96	30.27	928.91	0.03252	0.079
60.49	60.98	30.20	930.63	0.03255	0.080
60.43	60.89	30.29	932.32	0.03233	0.075
60.42	60.91	30.38	934.84	0.03213	0.080
60.38	60.94	30.36	932.48	0.03219	0.092
60.37	60.90	30.42	927.07	0.03231	0.088
60.37	60.88	30.45	925.56	0.03233	0.083
60.33	60.91	30.51	925.98	0.03221	0.096
60.38	60.85	30.55	928.84	0.03211	0.076
60.33	60.82	30.48	930.46	0.03208	0.080
60.37	60.86	30.55	936.11	0.03185	0.081
60.29	60.81	30.62	936.27	0.03169	0.085
60.25	60.75	30.64	935.11	0.03166	0.083
60.21	60.72	30.66	934.86	0.03160	0.084
60.23	60.65	30.53	930.19	0.03193	0.070
60.19	60.75	30.23	925.74	0.03237	0.092

Table 24 The thermal efficiency of ETC with 13 μm Al fin absorber

T_{in} (°C)	T_{out} (°C)	T_{am} (°C)	G_t (W/m ²)	$(T_{in}-T_{am})/G_t$	η
31.00	33.48	27.20	844.64	0.00450	0.450
30.98	33.42	27.18	843.99	0.00451	0.443
30.96	33.43	27.15	845.91	0.00450	0.447
30.94	33.43	27.18	846.06	0.00445	0.451
30.93	33.42	27.17	846.88	0.00444	0.449
30.93	33.37	27.18	844.24	0.00444	0.443
30.90	33.36	27.18	840.19	0.00442	0.449
30.88	33.35	27.19	840.64	0.00440	0.449
30.84	33.32	27.24	836.60	0.00431	0.453
30.83	33.29	27.27	839.09	0.00424	0.450
30.80	33.25	27.23	838.57	0.00426	0.447
30.79	33.26	27.21	843.08	0.00425	0.448
30.78	33.25	27.17	846.28	0.00427	0.447
30.74	33.19	27.18	838.40	0.00424	0.448
30.72	33.16	27.16	838.51	0.00424	0.446
30.70	33.14	27.15	839.06	0.00422	0.447
30.69	33.12	27.17	836.53	0.00421	0.446
30.66	33.11	27.20	835.72	0.00414	0.448
40.06	42.11	30.07	888.64	0.01124	0.354
40.54	42.67	30.74	908.61	0.01079	0.360
40.33	42.53	30.52	905.70	0.01083	0.372
40.45	42.46	30.49	883.82	0.01127	0.347
40.16	42.33	29.54	903.85	0.01175	0.368
40.22	42.28	29.58	904.66	0.01176	0.349
40.07	42.24	29.58	907.89	0.01155	0.366
40.10	42.21	29.55	908.21	0.01161	0.357
40.01	42.12	29.51	904.23	0.01160	0.359

Table 24 (cont.)

T_{in} (°C)	T_{out} (°C)	T_{am} (°C)	G_t (W/m ²)	$(T_{in}-T_{am})/G_t$	η
40.59	42.64	29.98	907.58	0.01169	0.347
40.14	42.35	29.91	909.97	0.01124	0.372
40.23	42.25	30.00	907.15	0.01127	0.340
40.10	42.18	29.95	904.83	0.01121	0.353
40.47	42.54	30.07	901.54	0.01153	0.352
40.30	42.31	30.04	887.94	0.01155	0.347
40.10	42.10	30.01	890.18	0.01133	0.343
40.06	42.11	30.07	888.64	0.01124	0.354
40.13	42.14	30.11	891.44	0.01124	0.344
50.53	51.77	28.87	922.13	0.02349	0.205
50.38	51.66	28.88	920.80	0.02335	0.213
50.32	51.59	28.97	921.56	0.02316	0.212
50.23	51.52	29.09	930.40	0.02272	0.211
50.12	51.40	28.97	934.05	0.02265	0.210
50.05	51.35	28.86	935.32	0.02266	0.212
50.53	51.73	28.82	922.30	0.02354	0.198
50.57	51.73	28.86	919.57	0.02360	0.194
50.51	51.67	28.89	920.33	0.02348	0.194
50.50	51.68	28.85	921.80	0.02348	0.196
50.38	51.54	29.01	921.54	0.02319	0.193
50.34	51.57	28.98	921.21	0.02319	0.205
50.30	51.48	28.97	921.96	0.02313	0.196
50.33	51.59	29.00	922.49	0.02313	0.208
50.12	51.39	28.82	935.76	0.02276	0.207
50.05	51.24	28.82	920.36	0.02307	0.197
50.01	51.27	28.89	936.30	0.02256	0.206
50.02	51.24	28.99	920.15	0.02286	0.202

Table 24 (cont.)

T_{in} (°C)	T_{out} (°C)	T_{am} (°C)	G_t (W/m ²)	$(T_{in}-T_{am})/G_t$	η
60.14	60.37	27.47	918.73	0.03556	0.039
60.08	60.39	27.72	919.20	0.03521	0.052
60.33	60.62	27.82	922.53	0.03524	0.047
60.36	60.62	27.82	922.58	0.03527	0.043
60.33	60.60	27.82	921.96	0.03526	0.045
60.41	60.65	27.89	919.51	0.03536	0.040
60.28	60.64	27.67	923.48	0.03532	0.060
60.28	60.60	27.76	922.27	0.03526	0.053
60.26	60.51	27.67	923.14	0.03530	0.042
60.63	60.89	28.15	922.71	0.03520	0.043
60.67	60.97	28.14	923.06	0.03525	0.050
60.58	60.88	28.38	921.04	0.03496	0.050
60.57	60.86	28.35	922.86	0.03492	0.047
60.49	60.83	28.30	916.74	0.03511	0.056
60.49	60.82	28.27	919.36	0.03504	0.055
60.50	60.84	28.30	918.93	0.03505	0.056
60.54	60.79	28.37	920.57	0.03494	0.043
60.66	60.95	26.93	954.32	0.03534	0.047

Table 25 The thermal efficiency of ETC with 11 μm Al fin absorber

T_{in} (°C)	T_{out} (°C)	T_{am} (°C)	G_t (W/m ²)	$(T_{in}-T_{am})/G_t$	η
30.77	33.84	28.18	898.91	0.00288	0.523
30.70	33.72	28.15	908.04	0.00281	0.510
30.60	33.54	28.03	883.97	0.00291	0.508
30.94	33.86	28.49	857.97	0.00284	0.523
30.88	33.81	28.51	861.70	0.00275	0.522
30.83	33.77	28.52	879.00	0.00262	0.513
30.78	33.68	28.48	871.38	0.00264	0.510
30.67	33.63	28.31	862.54	0.00274	0.524
30.65	33.55	28.28	871.10	0.00272	0.510
30.62	33.54	28.31	874.19	0.00264	0.511
30.58	33.51	28.36	864.83	0.00257	0.519
30.56	33.50	28.39	868.71	0.00251	0.517
30.50	33.35	28.71	857.55	0.00209	0.510
30.50	33.32	28.64	848.34	0.00219	0.509
30.51	33.36	28.61	846.30	0.00224	0.516
30.52	33.35	28.63	838.48	0.00226	0.517
30.53	33.35	28.64	829.64	0.00227	0.521
30.54	33.32	28.66	833.13	0.00226	0.511
40.34	42.43	28.14	909.12	0.01342	0.353
40.33	42.32	28.21	911.49	0.01329	0.334
40.24	42.29	28.25	910.94	0.01317	0.344
40.07	42.22	28.33	910.66	0.01289	0.361
40.21	42.27	28.30	908.73	0.01311	0.347
40.06	42.10	28.33	909.48	0.01290	0.344
40.01	42.18	28.35	910.17	0.01281	0.365
40.11	42.17	28.38	909.12	0.01290	0.347
40.16	42.12	28.43	910.98	0.01288	0.330
40.22	42.22	28.57	909.83	0.01280	0.336

Table 25 (cont.)

T_{in} (°C)	T_{out} (°C)	T_{am} (°C)	G_t (W/m ²)	$(T_{in}-T_{am})/G_t$	η
40.23	42.16	28.64	910.15	0.01273	0.325
40.09	42.19	28.48	912.32	0.01272	0.352
40.10	42.25	28.59	913.43	0.01260	0.361
40.06	42.13	28.58	911.79	0.01259	0.348
40.06	42.08	28.21	907.68	0.01306	0.340
40.83	42.96	28.61	904.98	0.01351	0.361
40.58	42.70	28.79	904.14	0.01303	0.361
40.74	42.71	28.90	903.91	0.01310	0.333
50.24	51.41	28.05	915.79	0.02423	0.197
50.22	51.37	28.05	931.86	0.02379	0.188
50.27	51.38	28.11	919.84	0.02409	0.185
50.28	51.44	28.08	933.78	0.02377	0.190
50.33	51.52	28.17	946.48	0.02341	0.194
50.69	51.89	28.23	946.97	0.02371	0.195
50.66	51.87	28.53	936.44	0.02363	0.197
50.64	51.83	28.56	937.35	0.02356	0.194
50.64	51.83	28.48	936.58	0.02366	0.195
50.64	51.83	28.44	938.01	0.02367	0.195
50.67	51.85	28.37	942.32	0.02366	0.192
50.65	51.78	28.42	924.67	0.02403	0.188
50.65	51.81	28.34	931.70	0.02394	0.191
50.64	51.82	28.35	930.50	0.02396	0.194
50.63	51.82	28.37	938.87	0.02371	0.194
50.79	51.91	28.51	918.54	0.02425	0.188
50.64	51.77	28.29	920.34	0.02429	0.188
50.67	51.77	28.35	914.22	0.02441	0.184
60.01	60.32	30.71	893.23	0.03281	0.052
60.02	60.40	31.37	878.20	0.03262	0.067

Table 25 (cont.)

T_{in} (°C)	T_{in} (°C)	T_{in} (°C)	T_{in} (°C)	T_{in} (°C)	T_{in} (°C)
60.12	60.42	31.38	870.61	0.03302	0.053
60.18	60.54	31.43	888.51	0.03236	0.063
60.18	60.52	31.46	889.07	0.03230	0.059
60.15	60.50	31.49	887.10	0.03231	0.060
60.20	60.52	31.48	887.62	0.03235	0.055
60.18	60.57	31.54	890.49	0.03216	0.066
60.23	60.55	31.50	887.55	0.03237	0.055
60.17	60.58	31.49	891.87	0.03215	0.070
60.26	60.55	31.49	898.97	0.03200	0.049
60.17	60.57	31.49	899.52	0.03189	0.067
60.24	60.59	31.50	904.68	0.03177	0.060
60.30	60.62	31.50	905.42	0.03180	0.054
60.30	60.63	31.53	905.49	0.03177	0.055
60.27	60.71	31.59	905.08	0.03169	0.075
60.34	60.69	31.57	910.82	0.03158	0.060
60.34	60.70	31.53	916.97	0.03142	0.060

APPENDIX E

The Parameter of annual energy calculation

$$T_a (^{\circ}\text{C}) = 30 \quad T_i (^{\circ}\text{C}) = 35 \quad T_o (^{\circ}\text{C}) = 60$$

$$G_t = 800 \quad E \text{ (kWh/m}^2\text{)} = 1800$$

Table 26 The calculation of annual energy calculation

thickness (μm)	Thermal efficiency equations	$c_o = F_R(\tau\alpha)_n$	F_R	$F_R U_L = c_I$	U_L	η	Annual energy yield (kWh/m ²)
11	$\eta = 0.5535 - 15.738x - 14.23x^2$	0.5535	0.65	15.74	24.32	0.45	818.25
13	$\eta = 0.5045 - 13.205x + 6.941x^2$	0.5045	0.59	13.21	22.39	0.42	758.62
24	$\eta = 0.3782 - 8.815x - 14.435x^2$	0.3782	0.44	8.82	19.94	0.33	598.58